UNIVERSIDADE DE LISBOA
FACULDADE DE CIÊNCIAS
DEPARTAMENTO DE BIOLOGIA ANIMAL

The control of cardiomyocyte proliferation by Cerl2 protein

Maria de Fátima Leitão da Silva

Mestrado em Biologia Evolutiva e Do Desenvolvimento

Dissertação orientada por:
Professor Doutor José António H. Belo
Professora Doutora Maria Gabriela Rodrigues

2019

Acknowledgements

Firstly, I would like to say thank you to Professor José Belo for the opportunity to be a part of his team and to develop this project. Also, for all the support, guidance and discussions that led to the conclusion of this work. I would also like to thank Professor Gabriela Rodrigues for the relevant feedback in the written work and the incredible support during the first year of this master's degree.

A very special thanks to José Inácio, for all the support and patience to teach me all the experimental techniques and for the motivation that eventually led to the conclusion of this project. I would also like to thank him for the revisions and comments during the writing of this dissertation.

I would also like to thank the members of this team during most of my time in the lab: Fernando Cristo, Oriol Bover, Sara Marques, Tiago Justo and Paulo Pereira.

A huge thank you for the support of my family, especially my mum. I could not do this without her. I would also like to thank my friends for supporting me in the conclusion of this work and for making life so much better. Thank you, André, Catarina, Norberto and Diogo.

Resumo

O desenvolvimento embrionário tem fascinado cientistas e filósofos desde a primeira descrição de Aristóteles sobre a fertilização e o desenvolvimento embrionário até à descoberta dos diferentes mecanismos genéticos e moleculares da atualidade. A Embriogénese é um mecanismo extremamente complexo que envolve interações temporais e espaciais entre milhares de células e moléculas. Começa com a fecundação de um oócito feminino por um espermatozoide masculino, que gera o zigoto. O zigoto sofre múltiplas divisões e rearranjos espaciais num processo chamado de gastrulação. As diferentes células diferenciam-se e especializam-se em três folhetos embrionários: endoderme, mesoderme e ectoderme. Estes vão sofrer rearranjos – morfogénese; e formar órgãos – organogénese; que eventualmente darão origem a um ser completo com capacidade de se reproduzir. Qualquer mínima falha neste processo pode desencadear uma cadeia de consequências, desde pequenas malformações até, em casos críticos, à inviabilidade do embrião e consequente morte.

Os animais apresentam vários tipos de morfologia corporal, devido à formação de órgãos com várias funções e diferente posicionamento durante a embriogénese. Nos vertebrados, o coração é o primeiro órgão a ser formado para poder fornecer oxigénio e nutrientes essenciais ao embrião em desenvolvimento. Para a sua morfogénese, várias vias de sinalização moleculares necessitam de estar intimamente relacionadas entre si. Falhas neste processo levam ao surgimento de doenças cardíacas congénitas. Durante o desenvolvimento embrionário, são vários os mecanismos que determinam o correto posicionamento deste e de todos os outros órgãos através da origem sequencial dos três principais eixos: o Anterior-Posterior (A-P), o Dorso-Ventral (D-V) e o Esquerdo-Direito (E-D). Este último é responsável, entre outras coisas, pelo posicionamento do coração na caixa torácica e pela correta morfologia dos ventrículos e das aurículas. Uma das principais vias de sinalização nesta fase do desenvolvimento, é a do Nodal. Nodal é uma proteína secretada pertencente à superfamília de fatores de crescimento β (TGF-β) que medeia a diferenciação inicial da mesoderme e é fundamental para a formação da linha primitiva e do nó na futura parte posterior do embrião. A formação destas duas estruturas marca o início do desenvolvimento do eixo A-P e D-V. O nó é uma estrutura transiente que tem um papel organizacional na formação do terceiro eixo, o E-D. As células ciliadas deste organizador do nó criam um movimento de rotação unidirecional que provoca o deslocamento de Nodal para o lado esquerdo do nó, onde vai interagir com várias proteínas antagonistas que vão limitar a sua expressão à Placa Lateral Esquerda da Mesoderme (PLEM). Esta expressão assimétrica de Nodal será a primeira quebra na simetria do embrião e levará ao correto posicionamento e formação do primeiro órgão assimétrico, o coração. Qualquer mutação que afete os genes desta cascata de sinalização, poderá levar a defeitos de lateralidade.

Com o objetivo de tentar compreender as patologias resultantes de anomalias na lateralidade presentes em humanos, foram desenvolvidos vários estudos e modelos animais, como ratinhos *knockout* para o gene *Cerberus-like 2* (*Cerl2)*. Cerl2 é uma proteína da família Cerberus/Dan conhecida por antagonizar moléculas da família TGF-β/Nodal. Em ratinho, Cerl2 é expresso assimetricamente nas células do lado direito do nó, onde a sua atividade modula o sinal de Nodal, restringindo-o à PLEM. A ausência da sua atividade antagonista causa uma sinalização anormal de Nodal no lado direito que desencadeia uma série de defeitos de lateralidade, tais como *situs inversus* (inversão da posição dos órgãos) e isomerismo (duplicação dos lados esquerdo ou direito).

Um estudo no nosso grupo revelou que aproximadamente 40% dos ratinhos KO para *Cerl2* apresentam vários defeitos de assimetria esquerda-direita. A maioria deve-se a problemas cardíacos, tais como falha na orientação do eixo cardíaco (looping randomizado), na formação do septo ventricular e auricular, transposição das grandes artérias e hipertrofia ventricular. Todos estes defeitos levam à inviabilidade do embrião ou morte à nascença. De forma a verificar independentemente qual seria o papel de *Cerl2* na formação dos defeitos cardíacos, foram selecionados ratinhos que não apresentavam defeitos de assimetria. Verificou-se então que estes apresentavam um aumento significativo no miocárdio compacto da parede dos ventrículos, bem como uma redução do pico de velocidade da artéria pulmonar e uma diminuição do ritmo cardíaco em relação à população *wild-type* (WT). O aumento do miocárdio foi associado a uma maior proliferação dos cardiomiócitos devido à ocorrência de a um maior índice mitótico, evidenciado pelo aumento da expressão de uma proteína do ciclo celular. Este aumento verificou-se nos estádios embrionários 13 (E13), e 15 (E15) e pós-nascimento (P0). No entanto, a E15 o aumento foi menor, não sendo considerado estatisticamente significativo. A este aumento de proliferação foram também associados maiores níveis de pSMAD2 e β–catenina nuclear, sugerindo uma ação prolongada da sinalização TGF-β/Nodal e Wnt/β–catenina, das quais são intermediários. Sabe-se que estas vias estão associadas à proliferação de cardiomiócitos durante a cardiogénese e a sua inibição leva à diferenciação dos mesmos. Como tal, propomos que a ausência de Cerl2 desiniba estas vias e cause uma maior proliferação destas células ao longo do desenvolvimento do coração.

Para tentarmos desvendar este mecanismo de ação do Cerl2 e verificarmos que a proliferação é independente de outras vias ou células fora do miocárdio compacto do coração, isolámos cardiomiócitos de corações de embriões de ratinhos *Cerl2*$^{-/-}$ e WT nos estádios E13 e E15. Os cardiomiócitos isolados foram divididos em três placas de cultura para serem fixados a diferentes pontos no tempo: 1, 4 e 7 dias após o respetivo isolamento. Este passo era fundamental pois, se os cardiomiócitos dos ratinhos *Cerl2*$^{-/-}$ de facto proliferassem mais em cultura em relação aos WT, era importante saber durante quanto tempo o conseguiam fazer e em que quantidade. Para podermos avaliar a taxa de proliferação recorremos à técnica de imunofluorescência. Para tal, usámos um marcador de cardiomiócitos – α-actinina sarcomérica (α-actinin); e um marcador de proliferação - Ki67. A taxa de proliferação foi feita dividindo o número de células que eram positivas para ambos os marcadores (α-Act^{+}Ki67^{+}) pelas que só eram positivas para α-actinin. Verificámos que *in vitro*, os cardiomiócitos dos ratinhos *Cerl2*$^{-/-}$ no estádio E13 apresentavam uma percentagem significativamente maior de proliferação do que os WT em todos os dias analisados. A maior diferença encontrada foi de 14.50%, em média, para o primeiro dia em cultura. No estádio E15 verificámos uma diminuição significativa na proliferação em relação ao estádio anterior. Dentro de E15, entre WT e *Cerl2* KO verificámos uma diferença bastante significativa no primeiro dia. No entanto, não foram significativas nos restantes dias.

Estes resultados estão de acordo com estudos anteriores. *Cerl2* é expresso no coração até E13, o que corresponde à fase de maior índice mitótico encontrado. Em E15 os resultados também parecem sugerir haver uma diminuição na proliferação. Esta diminuição também se verifica *in vivo*, pois um dos picos de proliferação ao longo do desenvolvimento encontra-se entre E12-13. Verificamos que de facto há uma diferença na proliferação entre WT e *Cerl2* KO E15 no primeiro dia em cultura, mas que deixa de ser significante nos dias a seguir. Os resultados parecem corroborar a hipótese de que *Cerl2* é de facto o regulador das vias de sinalização da proliferação de cardiomiócitos e que a cascada de efeitos resultantes ainda é existente a E13. Estas vias serão possivelmente TGF-β/Nodal e Wnt/β-catenina como reportado anteriormente. A diminuição a E15 poderá ser explicada pela diminuição dos efeitos neste estádio do desenvolvimento que só é suficiente para manter a maior taxa de proliferação em um dia de cultura. De facto, sendo *Cerl2* expresso no coração só até E13, é de esperar que outras sinalizações levem à redução dos efeitos das vias de sinalização anteriores.

O estudo da proliferação de cardiomiócitos tem vindo a ser cada vez mais fundamental no desenvolvimento de soluções para doenças cardíacas. As doenças cardíacas são das principais causas de morte no mundo. O coração adulto é um órgão com pouca capacidade de regeneração.

DAND5 é o homólogo humano de *Cerl2* e foi recentemente associado a uma série de defeitos de assimetria em Portugal. Uma das pessoas portadoras de uma variação deste gene possui defeitos cardíacos. Esta descoberta poderá estar relacionada com os processos que levam aos defeitos cardíacos em ratinho. Esperamos que os resultados obtidos possam abrir caminho para possíveis métodos de proliferação de cardiomiócitos para usar em medicina regenerativa e compreensão de doenças congénitas humanas.

Palavras-chave: proliferação de cardiomiócitos, *Cerl2*, vias de sinalização, desenvolvimento coração, assimetria esquerda-direita, cultura *in vitro*

Abstract

Cerl2 is a protein of the Cerberus/Dan family known to antagonize molecules of the TGF-β/Nodal family. In mice, Cerl2 modulates Nodal signaling, contributing to the left-right asymmetry in the lateral mesoderm plate of the developing embryo. Knock-out mice (KO) for *Cerl2* show several left-right asymmetry defects that lead to embryonic lethality or death at birth. These mice also show a significant increase of the compact myocardium wall of the left ventricle, even in mice without laterality defects, suggesting that *Cerl2* has an important role in the developing heart. This increase is associated with a higher mitotic index and proliferation of cardiomyocytes. These cells show higher levels of pSMAD2 and nuclear β–catenin, suggesting an extended exposure of the TGF-β/Nodal and possibly Wnt/β–catenin signaling. These signaling pathways are associated to cardiomyocytes proliferation and its inhibition leads to their differentiation. As such, we propose that the absence of Cerl2 up-regulates these pathways and leads to an increase in cardiomyocyte proliferation in the developing heart. To better understand this *Cerl2* mechanism and confirm that the proliferation is regulated in the heart cells, we isolated cardiomyocytes from *Cerl2*$^{-/-}$ and wild-type (WT) mice at stages E13 and E15. We verified that in culture, E13 cardiomyocytes show a significantly increase in proliferation when compared to WT in all the days analyzed. In stage E15 we also observe a decrease in proliferation compared to the previous stage, but significant differences between both types were only found at one day after culture. These results mirror former studies and demonstrate that the cells regulate their own proliferation.

DAND5 is the human homologue of mouse *Cerl2* and it has been also recently associated with several body-axis asymmetry defects in Portuguese patients. We hope these results can lead us to future methods of cardiomyocytes proliferation for regenerative medicine and understanding of heart diseases.

Keywords: cardiomyocyte proliferation, *Cerl2*, signaling pathways, heart development, left-right asymmetry, *in vitro* culture

Contents

List of Tables

List of Figures

Abbreviations

A-P	Anterior-Posterior Axis
AVE	Anterior Visceral Endoderm
Cerl2	*Cerberus-like 2*
CHD	Congenital Heart Disease
CM	Cardiomyocyte
CNCCs	Cardiac Neural Crest Cells
CVD	Cardiovascular Disease
DEPC	Diethyl pyrocarbonate
DMEM	Dulbecco's Modified Eagle Medium
D-V	Dorsal Ventral Axis
DVE	Distal Visceral Endoderm
E	Embryonic Day
ECM	Extracellular Matrix
EMT	Epithelial-to-Mesenchymal Transition
Epi	Epiblast
FBS	Fetal Bovine Serum
FHF	First Heart Field
GSK3	Glycogen Synthase Kinase 3
ICM	Inner Cell Mass
KO	Knockout
LPM	Lateral Plate Mesoderm
L-R	Left-Right Axis
Nkx2.5	*NK2 Homeobox 5*
Non-CM	Non-cardiomyocyte
PBS	Phosphate-Buffered Saline
PE	Proepicardium

PrE	Primitive Endoderm
PS	Primitive Streak
PSC	Pluripotent Stem Cell
SHF	Second Heart Field
TE	Trophectoderm
TFs	Transcription Factors
TGF-β	Transforming Growth Factor type β
Wnt	Wingless/ Integrated Family Members
WT	Wild Type

Units

%	Percentage
ºC	Degree Celsius
mL	Milliliter
mg/mL	MiliGram per Mililiter
rpm	Rotations per Minute

1. Background

1.1 Early Mouse Development

Embryogenesis starts with fertilization, the fusion of a male spermatozoid with a female oocyte that generates a single cell, the zygote. The zygote is a totipotent cell capable of dividing into smaller cells that will differentiate and create an entire organism (Figure 1). After fertilization, the zygote is cleaved into 2, 8 and 16 smaller cells – the blastomeres, it loses pluripotency and, in the mouse, reaches the morula stage at around embryonic day 2.5 (E2.5) (Krupinski et al., 2011). From E3.5 to E4.5, after multiple mitotic divisions and a compaction process, it reaches the blastocyst stage. The blastocyst is composed of two different cell lineages: the trophectorderm (TE) and the inner cell mass (ICM) (Johnson & Ziomek, 1981). The TE encloses the ICM and is responsible for the attachment to the maternal uterine wall (E4.5) and the formation of the trophoblast to later generate the placenta. Several transcription factors (TFs) have been identified has involved in TE development, such as Cdx2 and Eomes (Marikawa and Alarcón, 2012). TFs can coordinate spatially and temporally the expression of many genes, making them master regulators of complex events, such as cell differentiation. The ICM cells will differentiate into the Epiblast (Epi) and the Primitive Endoderm (PrE) (Marikawa and Alarcón, 2010). NANOG and GATA6 have been identified has the earliest TFs markers for Epi and PrE, respectively (C.S. Simon, 2018). At the mid blastocyst stage, ICM cells will express either NANOG or GATA6 in the well-known salt and pepper pattern (Guoji Guo, 2010).The epiblast gives rise to the embryo and some extraembryonic structures while the PE cells contribute to the formation of the Distal Visceral Endoderm (DVE) (E4.2), predecessor of the Anterior Visceral Endoderm (AVE) (E5.7) (Takaoka and Hamada, 2012). At this stage in the DVE, the expression of the Nodal antagonists Lefty1 and Cerl1 is crucial to mark the establishment of the prospective anterior side of the embryo (Takaoka et al., 2011).

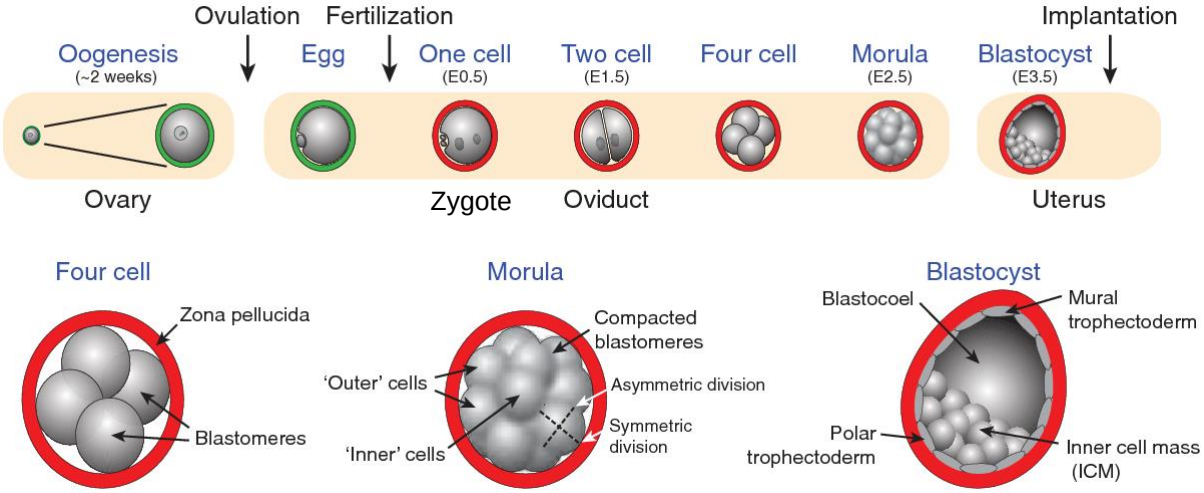

Figure 1: Overview of Early mouse development. Mammalian development starts at fertilization. The zygote goes through multiple cell divisions until it forms the blastocyst at E3.5. The blastocyst is composed by two different cell lineages - the Inner Cell Mass (ICM) and the Trophectoderm. The ICM will eventually generate the full embryo. (Adapted from Lei Li *et al*, 2010).

1.2 The establishment of the body axes

Animals have different body shapes with unique organ placement, morphology and function. Morphogenesis of the mouse embryo takes place during gastrulation and leads to the formation of the three germ layers – ectoderm, mesoderm and endoderm – that give rise to all type of tissues (Tam & Behringer, 1997). The formation of the germ layers combined with multiple cell division, fate specification and movement during embryogenesis, leads to the formation of three different body axes, the Anterior-Posterior axis (A-P), the Dorsal-Ventral axis (D-V) and the Left-Right axis (L-R).

1.2.1 The anterior-posterior and dorsal-ventral axis

Before gastrulation begins (E6), the AVE expresses *Cer1* (Belo et al., 1997), *Lefty1* (Meno et al., 1997) and *Dkk1* (Glinka et al., 1998), which inhibit Nodal and Wnt signaling in the anterior epiblast and restrict Nodal activity to the posterior, where the primitive streak (PS) will be formed (Kimura et al. 2000, Perea-Gomez et al. 2002). The PS is an elongated ridge of cells located at the midline of the early developing embryo and is fundamental for establishing bilateral symmetry, initiating germ layer formation and marking the site of gastrulation (Mikawa T, 2004). Epiblast cells undergo an epithelial-to-mesenchymal transition (EMT) to lose their epithelial characteristics such as cell-cell adhesion, and ingress through the PS to form mesoderm at the opposite side of the AVE, initiating the A-P axis development (Tam and Behringer, 1997; Beddington and Robertson, 1998, Nakaya & Sheng 2008, Nakaya et al. 2008, Nieto 2011). At the anterior side of the PS lie a few hundred cells, the node cells. The node is a transient structure that has an organizing role in the derivation of the primitive mesodermal structures and the notochord during early somitogenesis (Davidson & Tam, 2000). The notochord is important for the specification of cells in the central nervous system, somite formation, among others. The node therefore marks the formation of the second body axis, the D-V (Beddington and Robertson, 1999).

1.2.2 The Left-Right axis

Left-Right (L-R) asymmetry establishment is important for asymmetric organ morphogenesis and placement during embryogenesis. It requires three different events: breaking of the initial bilateral symmetry at the node, transfer of the LR-biased signal from the node to the lateral plate mesoderm (LPM) and asymmetric gene expression of signaling molecules that lead to the LR asymmetric positioning and morphogenesis of the internal organs (Shiratori & Hamada, 2014).

In the developing mouse embryo, the control of the L-R axis development is mainly achieved by the Nodal signaling pathway in the node, the L-R organizer. The *Nodal* genes are produced symmetrically in the crown cells of the node during early gastrulation. At head fold (E7.5), the ciliated motile pit cells from the node create a clockwise rotational movement towards the left side of the lateral plate mesoderm (LPM) - the leftward unidirectional Nodal flow (Hamada, 2008; Hamada et al., 2002; Hirokawa et al., 2012). This marks the first step of the breaking symmetry event. At this stage, Cerl2 protein binds to Nodal and regulates its expression by restricting it to the LPM (Marques et al., 2004). When the LPM cells start asymmetrically producing Nodal, the second symmetry event occurs. The cells that receive

nodal signaling will adopt left-side morphology while the others will adopt right-side morphology (Shiratori & Hamada, 2006).

Nodal induces the transcription of three target genes: *Nodal* itself, *Lefty* and *Pitx2* (Shiratori et al. 2001). At the LPM, it regulates its expression in a positive-feedback loop and activates the expression of the Lefty genes. *Lefty1* and *Lefty2* are Nodal inhibitors and as a result form a negative feedback loop restricting Nodal expression spatially and temporally, respectively. *Lefty1* mutants have Nodal expressed bilaterally in the LPM and develop left isomerism (Meno C. et al, 1998). While *Lefty2* mutant mice will have an extended Nodal expression until 8-9 somite stage instead of the normal 6-7 somite stage (Meno C. et al, 2001). When Nodal expression in the LPM ceases, the main gene that regulates asymmetric organogenesis is the transcription factor Pitx2 (Logan et al. 1998; Yoshioka et al. 1998). Like Nodal and Lefty2, Pitx2 is expressed asymmetrically in the left LPM. Mice deficient in Pitx2 exhibit laterality defects in most visceral organs (Liu et al. 2012) such as pulmonary right isomerism.

1.3 Transforming Growth Factor type β superfamily

1.3.1 Nodal

Nodal is a member of the Transforming Growth Factor type β (TGF-β) superfamily of secreted signaling factors. Nodal plays an essential role in L-R axis establishment, mesoderm and endoderm induction as well as neural cell patterning during embryogenesis (Kawasumi et al., 2011). In fact, nodal-null mutants fail to generate the PS leading to a lack of proper mesoderm formation (Conlon et al., 1994).

After the first role of Nodal in A-P axis formation, Nodal is re-expressed in the node and then in the left LPM (Nakamura and Hamada, 2012) to help establish L-R development (Figure 2). Nodal pathway occurs through types I and II serine/threonine kinase receptors (Schier, 2009). It binds with heteromeric complex co-receptor Epidermal Growth Factor (EGF)-like and cysteine-rich domain (Cripto-FRL1-Cryptic, CFC) motifs, EGF-CFC. (Ten Dijke and Hill, 2004). Binding of Nodal to its receptors leads to the phosphorylation of receptor-associated Smads (R-Smad) Smad2 and Smad3. Then the phosphorylated receptors interact with the co-factor Smad4 to form a transcriptional complex which will translocate to the nucleus and together with transcription factors (FoxH1, Mixer) regulate the expression of downstream target genes (Shen, 2007), such as the Lefty genes. These are also members of this superfamily and have an important role in L-R development. During the nodal flow Lefty1 and Lefty2 act as spatial and temporal antagonists, preventing excessive Nodal expression and blocking its migration to the right LPM, through a negative feedback loop (Meno et al., 2001; Hamada et al., 2001). Other members of this superfamily include the Cerberus family that acts as an antagonist in the Nodal signaling pathway.

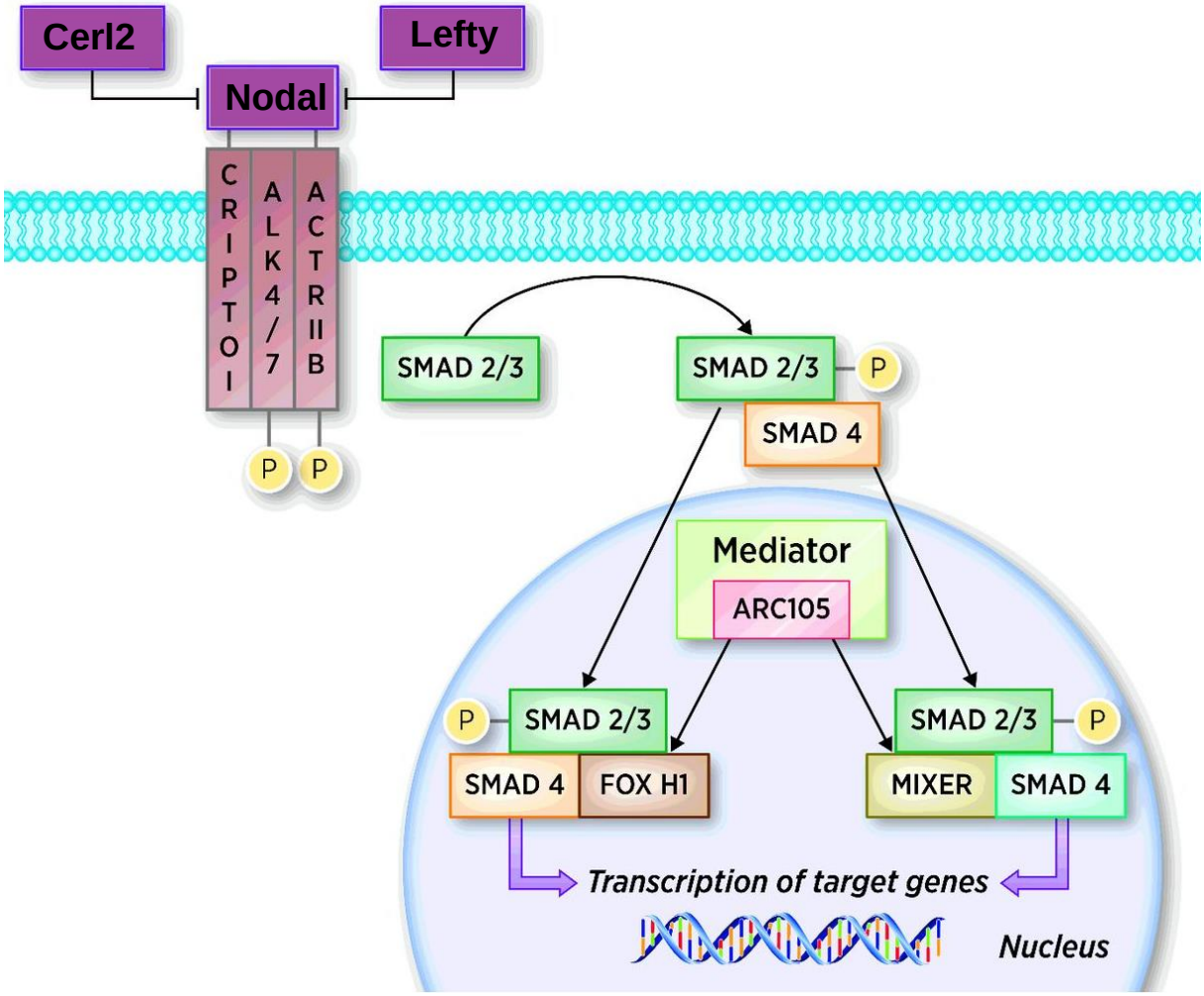

Figure 2: Nodal signaling pathway. Cerl2 and Lefty proteins inhibit Nodal allowing its asymmetric expression on the left side of the LPM. (Adapted from Kalyan et al., 2017).

1.3.2 Cerberus Family

The *Cerberus-like* (*Cer-l*) is a family of small secreted proteins – 272 a.a, Cerl-1 and Xcer and 185 a.a, Cerl2 - that belong to the TGF-β superfamily which are critically important for regulating cell development and growth and act as Nodal, BMP and Wnt protein antagonists (Belo et al., 1997; Marques et al., 2004). Cerl associated proteins have been found in several vertebrate species, such as the mouse mCerl1 (Belo et al., 1997) and mCerl2 (Pearce, 1999; Marques et al., 2004); chicken (cCerl1 or Caronte; Rodríguez Esteban et al., 1999), zebrafish (zCharon; Hashimoto et al., 2004) and humans (Dand5; Mouse Genome Informatics). The Cer-l family is characterized by 9 cysteines (Cystein-Rich Domain) at the C-terminal and a signal peptide at the N-terminal (Belo et al., 2009). Despite having a conserved cysteine-knot domain, the patterns of Cer-l expression is different between vertebrate species (Bouwmeester et al., 1996; Belo et al., 1997; Zhu et al., 1999).

Cerl1 equivalent in the *Xenopus* species (Xcer) was first identified in the yolky anterior endomesoderm at the Spemann's organizer (node equivalent in mouse) of its embryos. It acts as an antagonist to some signaling pathways in that region (Bouwmeester et al., 1996). The same study has shown that the injection of Xcer mRNA in blastomeres results in the formation of ectopic heads as well as duplicated internal organs (Bouwmeester et al., 1996). In mice, Cerl1 is expressed in the AVE and together with

Lefty-1 determines the establishment of the A-P axis restricting the PS to the prospective posterior side of the embryo (Belo et al., 1997; Belo et al., 2000; Yamamoto et al., 2004).

1.3.3 *Cerberus-like 2*

Cerberus-like 2 (*Cerl2*) is a member of the Cerberus/Dan family located on the chromosome 8 of the mouse. It encodes for a 20 k-Da secreted growth factor capable of antagonizing Nodal and therefore having an important role in the L-R axis formation during mouse gastrulation (Marques et al, 2004).

1.4 Cerl2 in L-R axis formation

Like Nodal, Cerl2 protein is also being bilaterally expressed in the crown cells of the node, in a horseshoe shape, like its mRNA. (Inácio et al, 2013). At the one-somite stage (E8), as soon as the leftward flow begins, it starts being asymmetrically expressed (L<R). This happens because *Cerl2* mRNA is post-transcriptional regulated via its 3'UTR (untranslated region) through Wnt signaling induced by Notch signaling becoming higher on the left-LPM, thus leading to Cerl2 degradation on the left side of the crown node cells (Nakamura et al., 2012; Kitajima et al., 2013). As *Cerl2* expression starts to become higher on the right side, Cerl2 proteins begin to accumulate on the right side of the node until 2-somite stage, preventing the activation of the Nodal cascade on the right-LPM. Therefore, nodal expression becomes higher on the L-LPM contributing to the beginning of L-R morphogenesis, starting with the rightward looping of heart at E8.5 At the 2-3 somite stage, Cerl2 protein begins being transported to the left side of the node in a nodal flow dependent way. This finding suggests that due to the protein's small size, it is being transported with the nodal flow (Inácio et al., 2013). Cerl2 protein is accumulated on the left side of the node from 5 until 6-somite stage when its expression ceases. This dynamic right-to-left translocation of Cerl2 protein seems to shutdown Nodal activity on the left side of the node at the 6-somite stage, which coincides with the termination of the Nodal expression and activity in the left LPM. The absence of Cerl2 antagonism in the node will result in a dosage-dependent randomization of Nodal signaling.

In the absence of Cerl2, Nodal expression in the node becomes randomized. As discussed above, the normal expression pattern of Nodal occurs in the L-LPM only. This expression can be inversed and found only on the R-LPM, known as *situs inversus*. Nodal can also be expressed bilaterally or be fully absent, a condition known as right *isomerism* (Belo, Marques & Inácio, 2017).

1.5 Cardiogenesis

1.5.1 Mesoderm induction

The mesoderm can be divided into four regions: chordamesoderm, paraxial mesoderm, intermediate mesoderm and lateral plate mesoderm. During cardiogenesis, the LPM splits into splanchnic and somatic layers, which will migrate into the heart contributing to the three main cell lineages, the endocardium, myocardium and epicardium (Buckingham et al., 2005).

Mesoderm induction requires the expression of Nodal and bone morphogenetic protein (BMP) signals as well as Wnt and fibroblast growth factors (FGF) (Kimelman 2006; Noseda et al. 2011). Mesodermal cells start ingressing through the PS when the expression of the T-box transcription factor Brachyury/T (Bry), a direct target gene of Wnt/β-catenin signaling begins. Commitment to a cardiogenic fate requires inhibition of canonical Wnt/β-catenin signaling and activation of noncanonical Wnt signaling (Gessert and Kuhl 2010).

1.5.2 Cardiac progenitors

Three precursor populations have been identified to contribute to different myocytic and non-myocytic cell lineages of the heart: cardiogenic mesoderm cells, the proepicardium (PE), and cardiac neural crest cells (CNCCs). (Brade T. et al, 2013).

1.5.3 Cardiogenic mesoderm cells

The cardiac mesoderm progenitors are among the first cells to ingress through the PS during gastrulation. After ingression these cells migrate to an anterior lateral position caudal to the headfolds, the splanchnic mesoderm, to form the horseshoe shaped cardiac crescent at E7.5 (Buckingham et al 2005). At this stage of development, the first (FHF) and second (SHF) heart fields can be distinguished (Kelly et al. 2014).

FHF progenitor cells start differentiating toward cardiomyocytes and smooth muscle cells when exposed to cytokines of the BMP (Schultheiss et al. 1997) and FGF (Reifers et al. 2000) families as well as to inhibitors of the Wnt pathway (Marvin et al. 2001; Schneider and Mercola 2001; Tzahor and Lassar 2001; Noseda et al. 2011), while endodermal Sonic hedgehog signaling keeps SHF progenitors in a proliferative state. The SHF progenitors can be divided in two sub-populations. Both will differentiate into smooth muscle cells, but one will also provide endothelial cells while the other will provide cardiomyocytes and contribute to the proepicardial lineages.

The expression of *Nkx2.5* (Lints et al. 1993), *Gata-4* (Arceci et al. 1993; Kelley et al. 1993; Heikinheimo et al. 1994; Zeisberg et al. 2005), and *Tbx5* (Harvey 2002) mark cardiac differentiation while the expression of contractile proteins such as myosin light chain-2a (Kubalak et al. 1994) and sarcomeric myosin heavy chain mark myocyte commitment.

1.5.4 Proepicardium

The early embryonic heart tube developing from the FHF and SHF progenitors consists of only two cell layers, the endocardium and the myocardium. The epicardium is the outmost layer of the heart and is not present at tubular heart stage. It's derived from a cluster of mesothelial cells developing at the base of the venous inflow tract of the early embryonic heart – the proepicardium. These cells give rise to the epicardium and the epicardium-derived cells (Manner et al. 2001). The latter undergo EMT and populate the myocardial wall, differentiating into smooth muscle cells, cardiac fibroblasts, endothelial cells and cardiomyocytes. Gata-4 is necessary for PE induction. PE cells and epicardium formation are absent in Gata-$4^{-/-}$ mice (Watt et al., 2004). Besides their role in myocardial wall formation and thickening, they also contribute to coronary vessel development.

The PE cells express several other transcription factors, such as TBX18, WT1, and TCF21, the competence factor for nodal-like signaling factors CFC, and the retinoic acid synthesizing enzyme RALDH2. Although none of these markers are uniquely expressed in the PE, the combinatorial expression of these markers is specific to the PE (Brade et al, 2013).

1.5.6 Cardiac Neural Crest Cells

CNCCs are a noncardiac subpopulation of the cranial neural crest cells that arise from the dorsal neural tube (Keyte and Hutson 2012). The crest cells delaminate from the neural tube and migrate towards the heart, reaching the pharyngeal arches 3, 4, and 6. Signals important for the induction of the CNC progenitors belong to the BMP/TGF-β superfamily of growth factors as well as to the FGF, Wnt/β-catenin, and retinoic acid signaling pathways (Hutson and Kirby 2007). They have an important role in providing signals for proper patterning of the aortic arteries, outflow tract (OFT) development and septation, and normal myocardial function. CNCCs differentiate into ectomesenchyme and aortic smooth muscle cells and form the aorticopulmonary septum, which divides the arterial outlet of the heart (Brade et al, 2013).

1.6 Heart formation

The heart is the first organ to be formed during organogenesis to supply the nourishment needs of the developing embryo (Guyton & Hall, 2011). The mammalian heart has four chambers. Two ventricles where blood is collected and pumped out of the heart and two atriums where blood enters the heart. Heart tissue needs to be supplied with oxygen and nutrients as well as a way of removing the metabolic wastes after consumption. This is achieved by the coronary circulation, which includes arteries, veins, and lymphatic vessels. These structures are all formed during development.

At E8, the cardiac crescent fuses at the midline and gives rise to the FHF-derived linear heart tube. The FHF (Pérez-Pomares et al., 2009) cells will contribute to the left ventricle (LV), atria ventricular canal, atria and inflow tract (Zaffran & Frasch, 2002; van den Berg et al., 2009). At E8.5 primitive circulation has been established (Kaufman & Bard 1999). The heart tube starts beating and undergoes rightward looping and rapid growth (Zaffran et al. 2004). Linear heart tube expansion requires cell proliferation and recruitment of additional cells. These additional cells come from the pharyngeal mesoderm and represent the SHF (Kelly 2012; Kelly et al. 2014). The SHF progenitors will contribute to the OFT, the right ventricle (RV), and a large portion of the inflow region (atria) (Waldo et al., 2005).

Freely floating PE cell vesicles are released and when on contact with the naked myocardium, form the epicardium between E9.5 and E11.5. Mesenchymal cells in the subepicardial space and in the myocardial wall will coalesce and differentiate, forming the primitive coronary plexus around E11.5 (Reese et al. 2002). Primary coronary vessels spread over the entire ventricle until E13.5. They will keep remodeling and differentiating as development progresses.

The full septation of the OFT and ventricles occurs at E13.5. The undivided OFT has three parts: aortic sac, truncus (arteriosus), and conus. They contribute to the outlets, valves, and bases of the aortic and pulmonary trunks. By E14.5 atrial septation is complete. Between E15.5 and E18.5 definitive external prenatal configuration is achieved (Savolainen, S. M. et al, 2009).

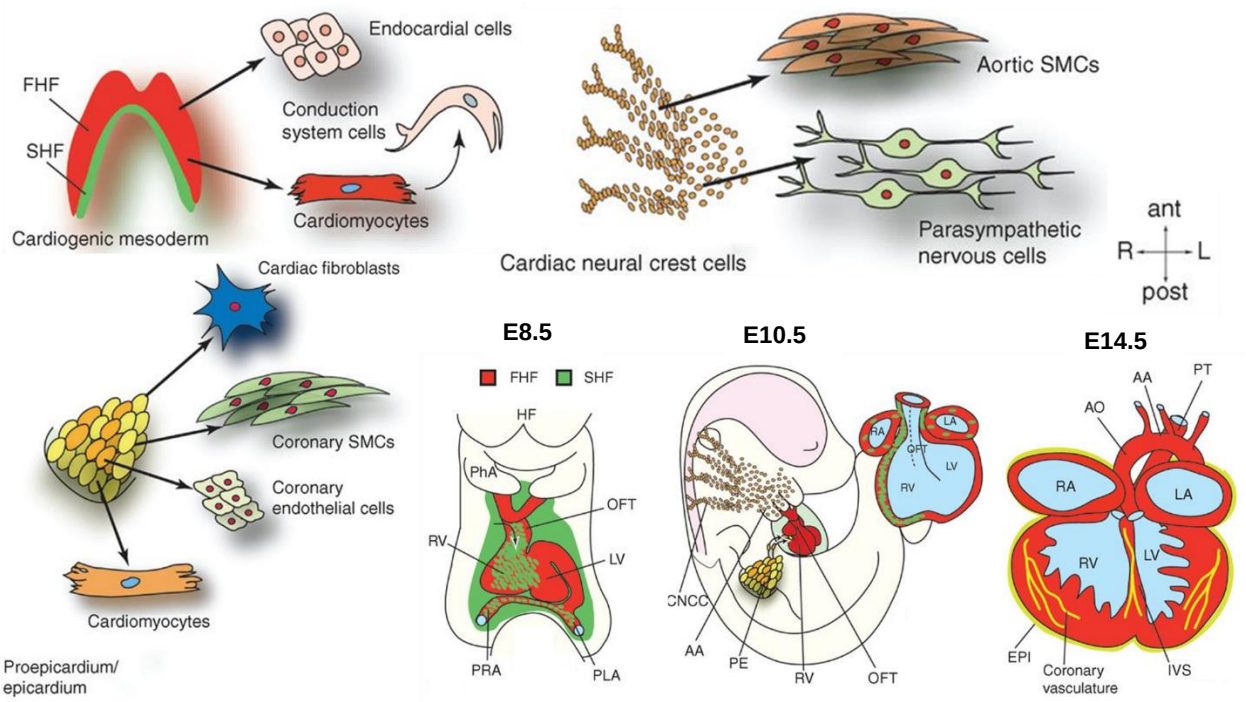

Figure 3: Embryonic heart progenitor contributions during cardiogenesis in mouse development. At E8.5, the linear heart tube undergoes rightward looping. At E10.5, cardiac neural crest and proepicardial cells start contributing to the heart, which already shows a defined four-chamber morphology. At E14.5, the heart shows four fully septated chambers and a septated outflow tract connected to the pulmonary trunk and the dorsal aorta. AA, Aortic arch; ant, anterior; AO, dorsal aorta; CNCC, cardiac neural crest cells; do, dorsal; EPI, epicardium; FHF, first heart field; HF, headfolds; IVS, interventricular septum; L, left; LA, left atrium; LV, left ventricle; OFT, outflow tract; PE, proepicardium; PhA, pharyngeal arch; PLA, primitive left atrium; post, posterior; PRA, primitive right atrium; PS, primitive streak; PT, pulmonary trunk; R, right; RA, right atrium; RV, right ventricle; SHF, second heart field; SMCs, smooth muscle cells; ven, ventral. (Adapted from Brade et al, 2013).

1.6.1 Cerl2 in heart formation

A study from our group reported that approximately 40% of the *Cerl2*$^{-/-}$ mice display L-R axis randomized and a significant mortality rate within a few hours after birth, mostly due to cardiac defects. Results showed a large increase in the myocardial walls of the left ventricle (LV) and intraventricular septum (IVS) even in the absence of other laterality defects (LD) (Marques et al., 2004). In order to assess the endogenous role of *Cerl2* in cardiogenesis, our team decided to analyze the cardiac

phenotypes presented in mice with no LD defects by crossing the *Cerl2* null mice with the Mlc1v-nlacZ-24 transgenic mouse line.

During cardiac looping (E8.5 – E10.5), the myocardium is composed of the trabeculae and the compact layer. (Ben-Shachar et al., 1985; Risebro & Riley, 2006). The trabeculae are myocardial projections into the chamber cavity outlined by endocardial cells. Their main function is to increase myocardial oxygenation in the absence of coronary circulation (Wessels and Sedmera 2003). The compact layer is an organized multilayer that comprises the outmost ventricular region beneath the epicardium and will form a thick compact zone of muscle (Ieda et al., 2010). Major increase in thickness of the ventricular wall, occurs between E11.5 and E14 (Kirby 2007), and it's the epicardium that maintains this proliferation (Chen et al. 2002). Cardiomyocytes that compose the compact layer have higher proliferative and lower differentiation capacities than the trabeculae cardiomyocytes (Rumiantsev & Bruce, 1991). During mid-gestation, (E12.5) the trabecular layer contributes, through condensation towards most of the increase in thickness of the compact myocardial wall (Wessels & Sedmera, 2003; Pennisi et al., 2003). At E13 in the *Cerl2*$^{-/-}$ mouse, right and left ventricular compact layer were shown to have the same thickness. They were also not significantly different from their respective WT counterparts. However, *Cerl2*$^{-/-}$ embryos were found to display increased LV trabecular expansion suggesting an increase in the compact layer after the compaction process. At E15, the LV compact myocardium is enlarged in the *Cerl2*$^{-/-}$ embryos, concluding that the mutant trabeculae cells contributed more significantly to the LV thickness (Araújo et al, 2014).

Heart tissue growth can be caused by an increase in cell number (hyperplasia) or in cell size (hypertrophy) (Hirschy et al, 2006). However, the major contribution to the heart size during the intrauterine period is due to high cardiomyocyte proliferation rate (Li et al., 1996; Sedmera and Thompson, 2011). Mitotic cardiomyocyte division peaks occur during mid-gestation (E12.5) and soon after birth (P3-P4) resulting in increased proliferation and binucleated cardiomyocytes formation, respectively (Soonpaa et al., 1996; Pasumarthi & Field, 2002). To assess if the LV increased thickness in the *Cerl2*$^{-/-}$ hearts were a result of hyperplasia or hypertrophy, proliferating cardiomyocytes were counted and the cardiomyocyte's relative area was measured. The results revealed an increase in mitotic index in the LV at E13 and P0 and no increase in relative cardiomyocyte area. They also showed an increase in *Cyclin D1* (*Ccnd1* in humans) relative mRNA cell expression (Araújo et al., 2014). Cyclin D1 is a cell cycle regulator necessary in the decision of the cell to progress to G1 phase during mitosis (Quelle et al., 1993). Therefore, we can conclude that the LV phenotype occurs due to cellular hyperplasia. At E15, although the mitotic index in the hearts of the *Cerl2*$^{-/-}$ embryos was found to be higher than in the WT embryos, it was not significantly different. It was also much lower than the previous mentioned stages as should be expected, because Cerl2 expression during heart formation occurs only until around E13 (Araújo A. et al, 2014).

pSmad2 and ß-catenin levels were also found to be elevated in the hearts of the *Cerl2*$^{-/-}$ E13 embryos and the neonatal mice. As mentioned before, pSmad2 is a mediator in the TGF-ß signaling cascade. In the absence of the Cerl2 antagonism, pSmad2 levels are higher and its effects seem to reach the neonatal stage, even though Cerl2 is only present in the heart until E13. Wnt/β-catenin canonical signaling pathway is implicated in early cardiovascular development (Buikema et al., 2013). A feedback loop between Wnt and Cerl2 is responsible for the generation of the signal asymmetry at the mouse node and Cerl2 is an inhibitor of the Wnt self-activating loop (Nakamura et al., 2012). Overall leading us to believe that the lack of Cerl2 in mice is associated with the dysregulation of both TGF-ß/Nodal, and Wnt/ß-catenin pathways, suggesting a possible role of Cerl2 in cardiomyocyte proliferation.

1.6.2 Cerl2 in the study of cardiac diseases

Cardiovascular diseases are a class of diseases that affect the heart or the blood vessels and are the biggest cause of death worldwide (Mendis S. et al, 2011). 45% of all deaths in Europe can be attributed to CVDs (Townsend et al, 2016). CVDs usually involve loss of myocardium due to oxygen and nutrient deficiency and replacement with non-contractile scar tissue (Coulombe et al., 2014). The main challenge in developing therapies for cardiac muscle repair is the limited regenerative capacity of the myocardium (Moran AE., 2014). The adult heart is composed of cardiomyocytes that have mostly lost the capacity to re-enter the cell cycle. The cell cycle is highly regulated and is comprised of several feedback loops that either allow or prevent cell division, depending on the cell type (Hydbring et al., 2016; Malum-bres and Barbacid, 2009). Mammalian cardiomyocytes can no longer enter the cell cycle soon after birth because they lose the ability to go through mitosis and cytokinesis (Naqvi et al. 2009). Recent studies have established that the heart contains a sub-population of multipotent stem cells capable of regenerating 1% of the cardiomyocytes found in the heart annually. However, they are not enough to compensate for the damage caused by most CVDs. Currently, the only treatment available to restore complete heart function is heart transplant (Moran AE., 2014). Heart transplants are very limited in resources and have several negative impacts in the human body due to the need of using immunosuppression therapies. Regenerative medicine approaches such as cardiac tissue engineering and cell-based therapies have been showcased as an attractive prospective in CVDs treatment.

Cardiac tissue engineering involves myocardium formation *in vitro* and its implantation at the site of injury to restore function to the diseased heart muscle tissue (Place ES., 2009). Having a viable source of human functionally mature cardiomyocytes and patient compatible is essential for both these applications. Human cardiomyocytes derived from pluripotent stem cells (PSCs) are the only viable source for new cardiomyocytes currently available. Therefore, it is important to establish new techniques and methods to increase cardiomyocyte proliferation *in vitro*. Cerl2 is known to be involved in major cardiomyocyte proliferation signaling pathways. Its use in the study of PSCs could contribute to develop larger number of cells to further develop therapies for CVDs.

Congenital heart diseases (CHD) is a defect in the structure of the heart or great vessels that is present at birth. CHD is the most common birth defect, affecting 0.4%–5% of live births. Around 30% of prenatal loss is due to heart mal formations (Hoffman 1995; Bruneau 2008). CHD most commonly arises from defective cardiac morphogenesis.

DAND5 is a Nodal antagonist that is involved in the correct L-R body axis establishment during gastrulation (Belo et al., 2017). Several variants of different genes involved in this signaling pathway have been associated with CHD (Deng et al., 2015). In a screening project designed to identify mutations associated with L-R asymmetry in humans, a new DAND5 heterozygous nonsynonymous variant c.455G>A was identified in a patient diagnosed with ventricular septal defect with overriding aorta, right ventricular hyper-trophy, and pulmonary atresia (Cristo et al., 2017). According to a functional analysis *in vitro*, this mutation leads to a decrease in the inhibitory function of the DAND5 protein. This suggests that, like *Cerl2* KO mice, human DAND5 fetuses with similar heart defects related to increased cardiomyocyte proliferation may have aborted or died at birth. Therefore, it is crucial to establish a disease model of this Cerl2 mutation to study its role in cardiovascular disease.

2. Objectives

Cardiovascular diseases have become the main cause of death in developed countries (Mendis S. et al, 2011). Cardiovascular diseases usually involve loss of myocardium and formation of non-contractile scar tissue that severely declines patients' wellbeing (Coulombe et al., 2014).
In the last decades, several studies have been done to develop an efficient protocol to derive cardiomyocytes from pluripotent and multipotent stem cells with the purpose to recover the damaged myocardium (Le et al., 2017). Cardiomyocytes are known to have a very limited proliferation capacity *in vitro*. Therefore, the study of signaling pathways involved in cardiomyocyte proliferation could lead to the development of several cardiac regeneration disease models.

Recent data from our group has shown that loss of function of *Cerl2*, leads to a massive increase of the ventricular walls in mice. This increase is due to a higher mitotic index of the cardiomyocytes of the compact myocardium (Araújo et al., 2014). An increase in the expression of key members of the TGF-β/Nodal/Wnt signaling pathways was also reported. These signaling pathways are known to be involved in cardiomyocyte proliferation and are known to be inhibited by Cerl2. Therefore, it is reasonable to hypothesize that the Cerl2 protein controls both signaling pathways in the heart during embryogenesis and is involved in the decision mechanism of cardiomyocyte proliferation.

Therefore, the main objectives of this work consist in:

1. Establishing and optimizing a protocol for embryonic cardiomyocytes isolation;

2. Establishing if the proliferation capacity of the *Cerl2* knockout cardiomyocytes is increased *in vitro* at E13 and E15.

3. Addressing the role of *Cerl2* as a key agent and interactor with the cardiomyocyte proliferation signaling pathways, TGF-β/Nodal and Wnt/β-catenin.

3. Materials and Methods

3.1 Mice

All animal work performed in this study was conducted compliant with the Portuguese law and approved by the Competitive Authority of the Veterinary Agency (Portuguese Ministry of Agriculture), the sole Agency/Committee in Portugal responsible to issue the ethical approval for these types of studies, following the EU guidelines for animal research and welfare.

All mice used in this experiment were WT and *Cerl2*$^{-/-}$ on background 129/Sv that had previously been generated by our team (Marques et al., 2004). The animals were housed in microisolator cages that were kept in an air-conditioned room at 22°C with a 12-hour light-dark cycle. They were fed with autoclaved mouse food and tap water.

Females were mate with males in the afternoon. Copulation usually occurs around midnight (Suckow et al., 2001), so in the following morning, vaginal plugs were checked to confirm successful mating. A vaginal plug is a whitish mass occluding the entrance of the mouse vagina and it's a consequence of the coagulation of some proteins present in the male mouse ejaculated semen (Suckow et al., 2001). This structure starts disappearing between 8 to 24 hours after copulation, so the vaginal plug detection was always performed before noon. Noon of the day of detection of the vaginal plug was considered as E0.5.

For this experiment we were looking for E13 and E15 mice embryos, so 13 and 15 days after plug detection, respectively, pregnant females were sacrificed by cervical dislocation. The uterine horns were immediately removed and placed in freshly filtered and autoclaved Phosphate Buffered Saline (PBS) DEPC at 4°C.

3.2 Isolation Protocol

Embryos were removed from their uterine horns gently and placed in a petri dish with PBS-DEPC at 4°C. Their heads were immediately removed with the help of sterile scissors and a sterile clamp. Since the higher mitotic index was only found in the cardiomyocytes of the ventricles (Araújo et al, 2014), the hearts were dissected from each embryo with the aorta, pulmonary artery and both atriums carefully removed. The remaining ventricles were then chopped with a sterile blade to facilitate enzyme digestion. For E13 we placed all the hearts from the same litter and blended them in MACS, using the m_hearth_01 program. For E15 we transferred each heart to a sterile Eppendorf tube. In both methods, the cells were incubated at 37˚C with a 2mg/mL collagenase solution containing 20% Fetal Bovine Serum (FBS). The ventricles were pipetted up and down with a 200mL tip in a laminar flow chamber. We found that this method was the best to prevent cell contamination and to better separate the heart cells. During this time, the process was repeated in intervals of 15 minutes until there were no visible heart tissues left. Approximately 30-60 minutes in E13 and 60 minutes plus for E15. Dulbecco's Modified Eagle Medium (DMEM): Nutrient Mixture F-12 at 37°C was added in the same volume as the collagenase solution to each tube and then they were centrifuged for 5 minutes at 850 rpm. The supernatant was removed, and the cells were resuspended in fresh culture medium.

3.3 Cell culture

Cells were then counted. With this method, approximately 226000 cells/mL were obtained. The recommended number of cardiomyocytes per well in a 24-well plate for 1000 mL of medium is between 15000-45000 (Buikema et al., 2013). In our experiment we found that 25000 cells per well generated a better overall result. The cells were divided and seeded in 3 separate 24-well plates with gelatinized-coated (1%) cover slips. Each plate to be fixated for immunofluorescence at 1, 4 and 7 days after culture. Medium changes were made every day or in alternating days.

3.4 Immunofluorescence

After removing the medium and washing 1x with PBS, cells were fixated with 4% paraformaldehyde (PFA) for 15 minutes at room temperature (RT). They were then washed with 1x PBS and permeabilized with 0,1% Triton for 30 minutes and finally blocked for another 30 minutes with 1% blocking solution at RT. The primary antibodies were added with the blocking solution (Table 1) for 2 hours RT or overnight (O/N) at 4°C. The cells were washed 3x for 5 minutes with 0,1% Triton. The secondary antibodies were added with blocking solution for 1 hour at RT. After a new 3x 5 minutes wash with 0.1% Triton, the coverslips were carefully mounted with Antifade Mounting Medium containing DAPI and sealed with nail polish to prevent drying and movement under the microscope.

Table 1: List of antibodies used in the immunofluorescence assays

Antibody	Dilution	Company
Mouse Monoclonal Anti-α-Actinin (Sarcomeric)	1:500	Sigma, A7811
Rabbit Polyclonal Anti-Ki67	1:500	Abcam, ab15580
Rabbit Polyclonal Anti-Vimentin	1:200	Abcam, ab137321
Alexa Fluor 488 – Donkey Anti-Rabbit	1:1000	Jackson ImmunoResearch
Alexa Fluor 594 – Donkey Anti-Mouse	1:1000	Jackson ImmunoResearch

3.5 Cell number analysis

The quantification of proliferating cardiomyocytes in each coverslip was performed by dividing the coverslip in 5 regions and randomly selecting an area of each one to count. Cell counting was performed manually with ZEN 3.0 (blue edition), a ZEISS software and automatically with an ImageJ plugin. Nuclei contained in α-actinin staining were considered individual cardiomyocytes while the other were considered non-cardiomyocyte cells. Nuclei positive for Ki67 were proliferating cells. The proliferating index/rate was obtained by dividing the number of proliferating cardiomyocytes ($\alpha\text{-Act}^{+}\text{Ki67}^{+}$) by the total number of cardiomyocytes ($\alpha\text{-Act}^{+}$). Images were taken in a Zeiss Axio Imager Z2 microscope at 20x magnification.

3.6 Statistical Analysis

Statistical analysis was performed using GraphPad Prism 8.2.0 version. Statistical differences were determined by unpaired two-tailed t-test with Welch's correction. We assumed that, given the same conditions, both WT and *Cerl2*$^{-/-}$ populations represent a normal distribution but do not have the same standard deviation. For this analysis, we did comparisons of cell proliferation rate, 1, 4 and 7 days after culture at E13 and E15 between WT and *Cerl2*$^{-/-}$. We also analyzed the differences between E13 and E15 proliferation rates in the same day after culture. P-value < 0.05 was considered statistically significant.

4.1 Results

4.1 Isolation of the E13 cardiomyocytes

To obtain the E13 cardiomyocytes, we needed to test and improve an efficient cell isolation protocol. The protocol started by carefully removing and chopping the ventricles of the hearts of E13 embryos. These embryos were obtained from E13 pregnant females. In total, this experiment required the use of 14 pregnant females. 9 females were WT and generated a total of 38 embryos, while the remaining 5 were *Cerl2* KO and generated a total of 30 embryos. After removing the ventricles, they were placed in a collagenase solution for enzymatic digestion. Collagenase is an enzyme capable of breaking the peptide bonds in collagen - the main structural protein in the extracellular matrix (ECM) produced by fibroblasts (Gerard J. et al, 2007). In the heart, the ECM preserves cardiac structure and function by maintaining cell shape, transmitting mechanical and contractile forces from individual myocytes for coordinated contractions, and regulating elastic recoil during cavity filling (diastole) and contraction (systole) (Rienks M. et al, 2014). Most myocardial collagen fibers consist of collagen types I and III (Ricard-Blum S., 2001). Collagenase does not harm the cell membrane, and has therefore been used in cell dispersion, tissue separation, and cell culture for many years (Villarreal, F, 2009). The ventricles were kept in the collagenase solution for different time periods. For assessing the cardiomyocyte proliferation rate, we only ended up successfully culturing and analyzing the cells from 3 WT and 3 *Cerl2* KO females, representing a success rate of 33,3% and 60% respectively. From these females we obtained 15 *Cerl2* KO and 23 WT embryos, respectively. The 8 unsuccessful cultures were mainly due to contamination and/or lack of initial experience. Despite all the material and solutions being sterile and filtered, the hearts had to be removed and placed on collagenase outside of a sterile chamber. The longer it took, the more likely it would be to get exposed to microorganisms. Over time and practice it stopped occurring. Another problem we had to face in the protocol was the lack of good cell separation due to poor mechanical disaggregation or a shorter time period in collagenase, which resulted in big lumps of beating cells. These couldn't be used because our interest was to see how isolated cardiomyocytes would act and proliferate in culture. We had to do several incubation periods and technical trials until we could get higher percentages of single isolated cardiomyocytes. We found that keeping them on the solution for 30-60 minutes while performing mechanical disaggregation by pipetting in intervals of 15 minutes was eventually the best approach. This was performed in a sterile airflow chamber. After neutralizing the collagenase solution with cell medium and counting the cells in a Neubauer chamber, the cells were cultured in 24 well plates coated with a gelatin solution for better growth and attachment. The highest number of cells obtained for used heart was 50,000. A previous study reported obtaining 50,000 – 200,000 cells per heart between E11.5-E14.5 (Buikema et al., 2013). For our experiment, it was important to analyze the cells at three different time points: 1, 4 and 7 days after culture. This was because it was not only important to verify if the cells proliferated more but also if they kept doing it even without other heart signals. So, the cells from the same hearts were separated into 3 different plates that would later be fixed for immunofluorescence.

4.2 Analysis of the E13 cardiomyocytes

To assess what type of cells were found in our cultures, we performed immunofluorescent assays for several known markers. For cardiomyocyte visualization we chose to use sarcomeric α-actinin. α-actinin is a 100kDa actin-binding protein that is found in muscle as well as non-muscle cells. In smooth muscle cells, α-actinin is present in dense bodies and plaques whereas in normal skeletal muscles, it is associated with z-discs that define muscle sarcomeres (Sorimachi H. et al, 1997). However, the antibody we chose was specific for α -skeletal and α-cardiac muscle actinins and doesn't react with non-skeletal muscle elements, such as connective tissue, epithelium, nerves and smooth muscle, making it the perfect choice for our study. These α-actinin positive (α-Act^{+}) cells also expressed Nkx2-5. Nkx2-5 is a homeodomain transcription factor expressed in precursor cardiac cells and is necessary for cardiomyocyte differentiation and proper cardiac development (Harvey RP, 1996).

After confirming the presence of the cardiomyocytes with the use of the α-actinin marker, there were still some cells left to identify. Staining for vimentin revealed than all non-cardiomyocytes cells, α-actinin negative (α-Act^{-}) were vimentin positive (vimentin^{+}) (Figure 4). Vimentin or fibroblast intermediate filament is the major intermediate filament found in non-muscle cells (Colvin et al., 1996). These cell types include fibroblasts, endothelial cells, macrophages, melanocytes, Schwann cells, and lymphocytes. Vimentin has also been demonstrated to be expressed in cardiac myofibroblasts. At this embryonic stage we should expect to find several types of cells, such as: cardiomyocytes and endothelial cells derived from mesodermal cells; cardiac fibroblasts and smooth muscle cells from the proepicardium. Therefore, it is possible that the vimentin^{+} cells are not only cardiac fibroblasts but also endothelial-type cells.

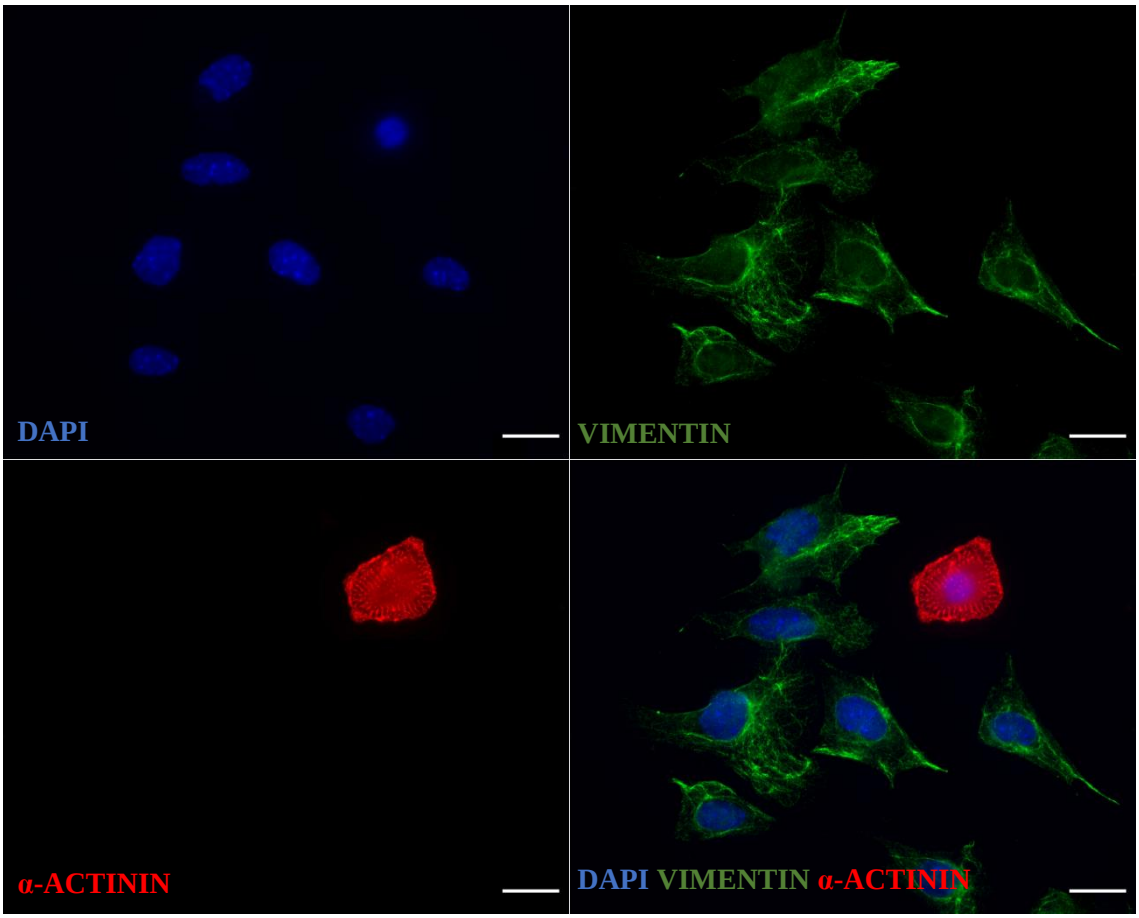

Figure 4: Cardiomyocytes and non-cardiomyocyte cells in culture. Immunofluorescence of cardiomyocytes from E13 *Cerl2* KO embryos at 1 day in culture. In the figure we can distinguish between an α-actinin positive cardiomyocyte (red) and several non-cardiomyocytes (green) that are vimentin positive. Bar, 20µm.

For the cardiomyocyte proliferation rate experiment, we needed to find a suitable proliferation marker. We tested our cultures for Ki67. Ki67 is a protein that is present during all active phases of the cell cycle (G1, S, G2 and M), but is absent in resting cells (G0) (Shirendeb U., et al 2009; Hooghe B., et al 2008). Its expression decreases during anaphase and telophase, later phases of mitosis (Modlin IM et al 2008). We found that this marker was suitable for our experiment, because it has a wide range of expression in the cell cycle. Also, we were not interested in any specific point of cell division, only to see if in fact it was occurring. In our immunofluorescence assays it was common to see sarcomere disassembly together with proliferating cardiomyocytes (α-Act^{+}Ki67^{+}) cells (Figure 5). In fact, there were some cardiomyocytes' nuclei that weren't Ki67^{+} but where we could still clearly see the sarcomere disassembly. These cells were not counted as being proliferating.

After identifying the type of cells found in our cultures, we decided to analyze their percentages at the different time points of the experiment. A previous study with a similar protocol had showed that non-myocytes are usually 40% of cells at day 1 and can increase up to 50-60% by day 3 (Buikema et al, 2013). In fact, α-Act^{+} cells represented 60% of the WT culture in day 1 (Figure 6). This percentage slightly increased on day 4 but came down on day 7. With some cultures reaching 38-40%. Surprisingly, *Cerl2* KO cultures had less α-Act^{+} cells than α-Act^{-}, averaging 36% on day 1. This value increased to 43.5% at day 4 and 47% at day 7. However, the results were not significantly different between the WT and the *Cerl2* KO cultures.

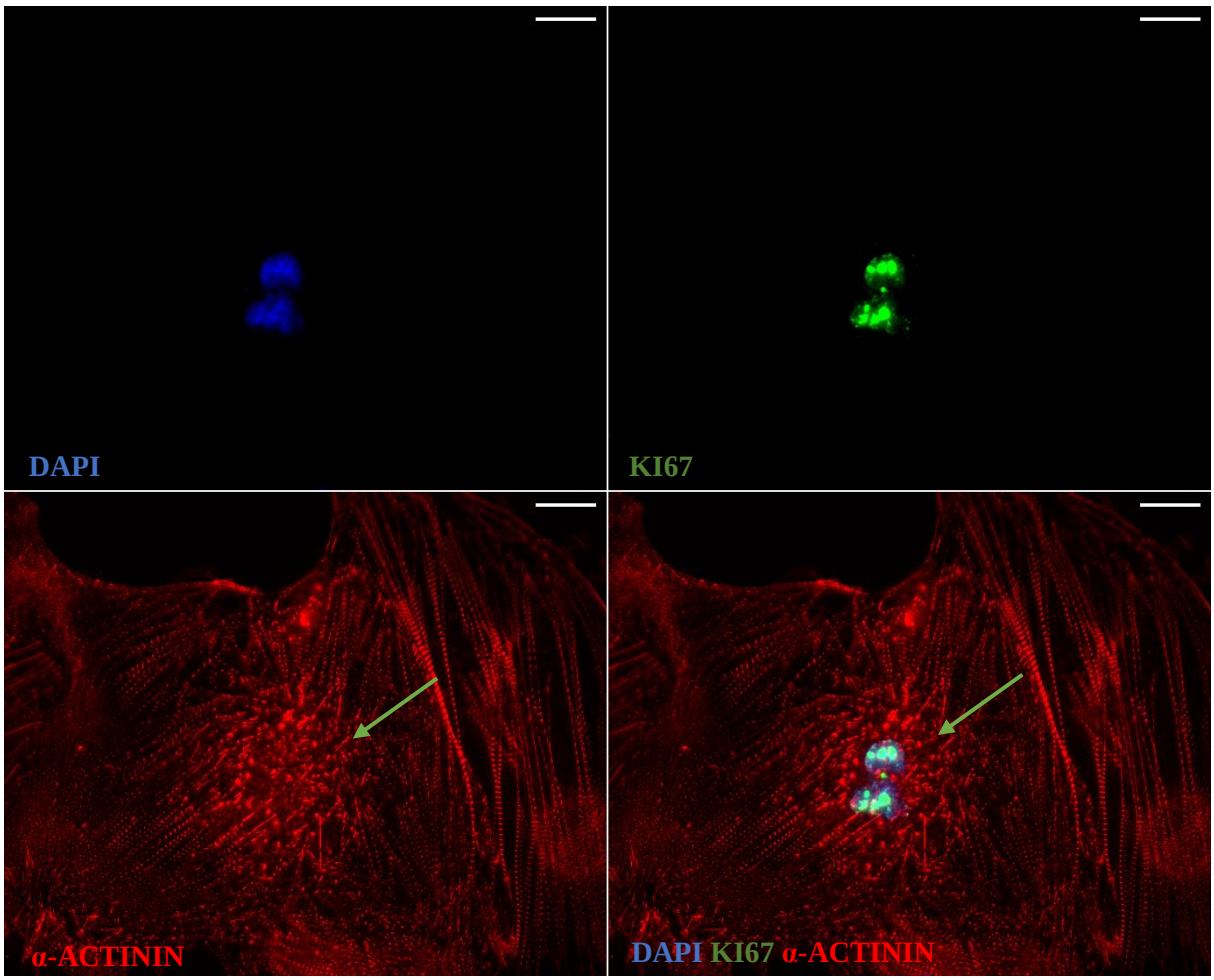

Figure 5: Sarcomeric disassembly during CM proliferation. Immunofluorescence of cardiomyocytes from E13 Cerl2 KO embryos at 4 days in culture. In the figure we can see 2 nuclei within a cardiomyocyte (α-Act^{+}) proliferating (Ki67^{+}) coupled with sarcomeric disassembly (arrow). Bar, 20µm.

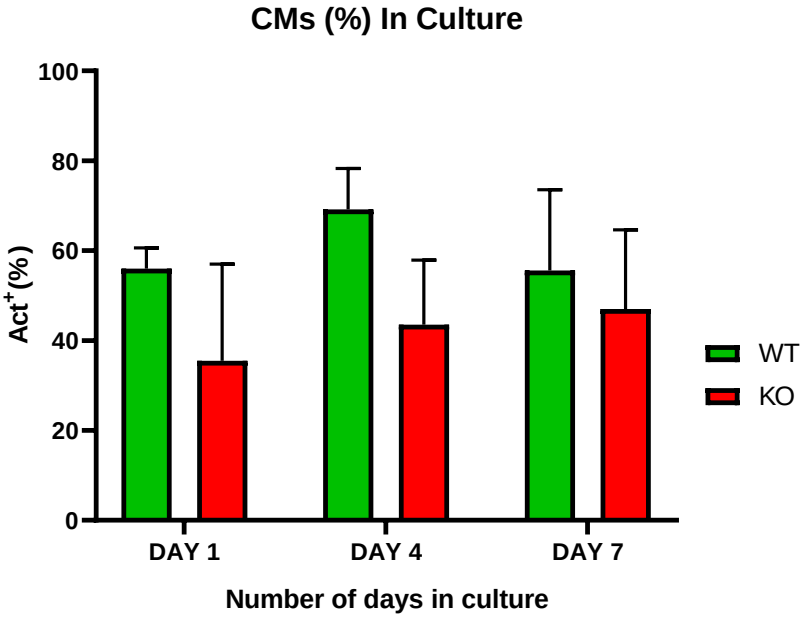

Figure 6: Cardiomyocyte percentage in culture. The figure shows the percentage of cardiomyocytes (Act+) from E13 *Cerl2* KO (red) and E13 WT embryos (green) at 1, 4 and 7 days in culture. Results show that there is a lower percentage of E13 *Cerl2* KO Act^+ cardiomyocytes present in culture at Day 1 (20.50%), 4 (19%) and 7 (8.6%) when compared to the E13 WT culture. However, no significant differences were found ($P<0.05$). Data is presented as mean ± SEM.

Since studying the cardiomyocytes proliferation rate was the most important part of our study, we found it would be interesting to analyze the percentage of proliferating non-cardiomyocytes cells (α-Act^-). We found that they are very similar on average in both WT and *Cerl2* KO cells (5% maximum difference on average). And their values keep decreasing from day 1 until day 7 (Figure 7).

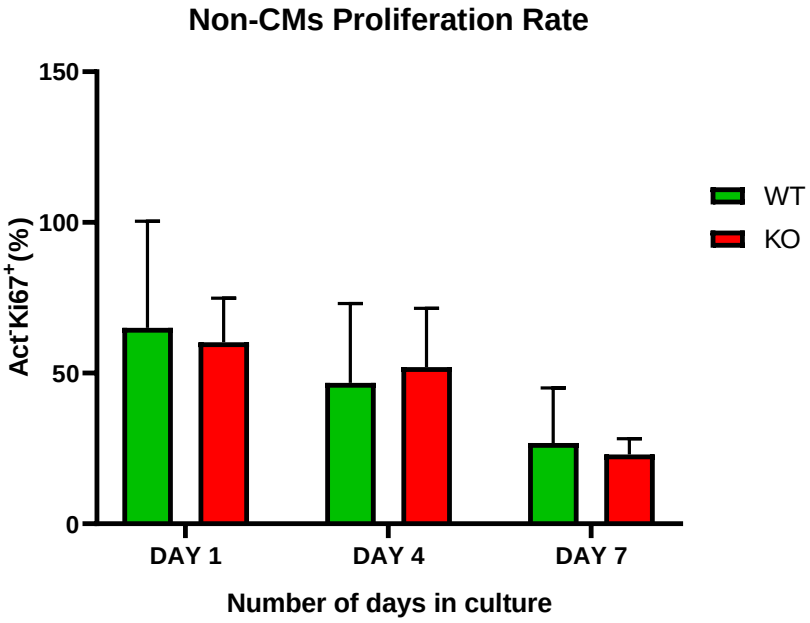

Figure 7: Non-cardiomyocyte proliferation rate in culture. The figure shows the percentage of proliferating non-cardiomyocytes (Act^-Ki67^+) from E13 *Cerl2* KO (red) and E13 WT embryos (green) at 1, 4 and 7 days in culture. Results show that non-cardiomyocytes proliferate more in culture on Day 1 (65% - WT; 60% *Cerl2* KO on average) than on Day 4 (47% - WT; 52% - *Cerl2* - KO) and Day 7 (27% - WT; 23% *Cerl2* KO). However, no significant differences were found between the two types ($P<0.05$). Data is presented as mean ± SEM.

4.3 E13 *Cerl2* KO cardiomyocytes have a significantly higher proliferation rate than WT cardiomyocytes

E13 *Cerl2* KO mice present a larger myocardium wall which is the result of an increase in the mitotic index of the cardiomyocytes of the ventricles (Araújo et al, 2014). This is the result of the lack of inhibition of *Cerl2* in the signaling pathways that control cardiomyocyte proliferation. Therefore, we found it important to assess cardiomyocyte proliferation *in vitro* and see if it compared to the results found in the developing embryo. We decided to start by analyzing the proliferation 1 day after culture (Figure 8). By this stage the cardiomyocytes had time to establish and bind to the coating gelatin but had not been out of the heart for too long. Day 4 (Figure 9) and 7 (Figure 10) were also tested because we wanted to see if they could continue having the same proliferation numbers in later days of culture. To assert the cell proliferation rate, we fixed our cells at the different time points and did an immunofluorescent assay. Proliferation rate was measured by dividing the number of $\alpha\text{-Act}^{+}\text{Ki67}^{+}$ cells with the total number of $\alpha\text{-Act}^{+}$ cells. All cell cultures were subjected to the same protocols and conditions.

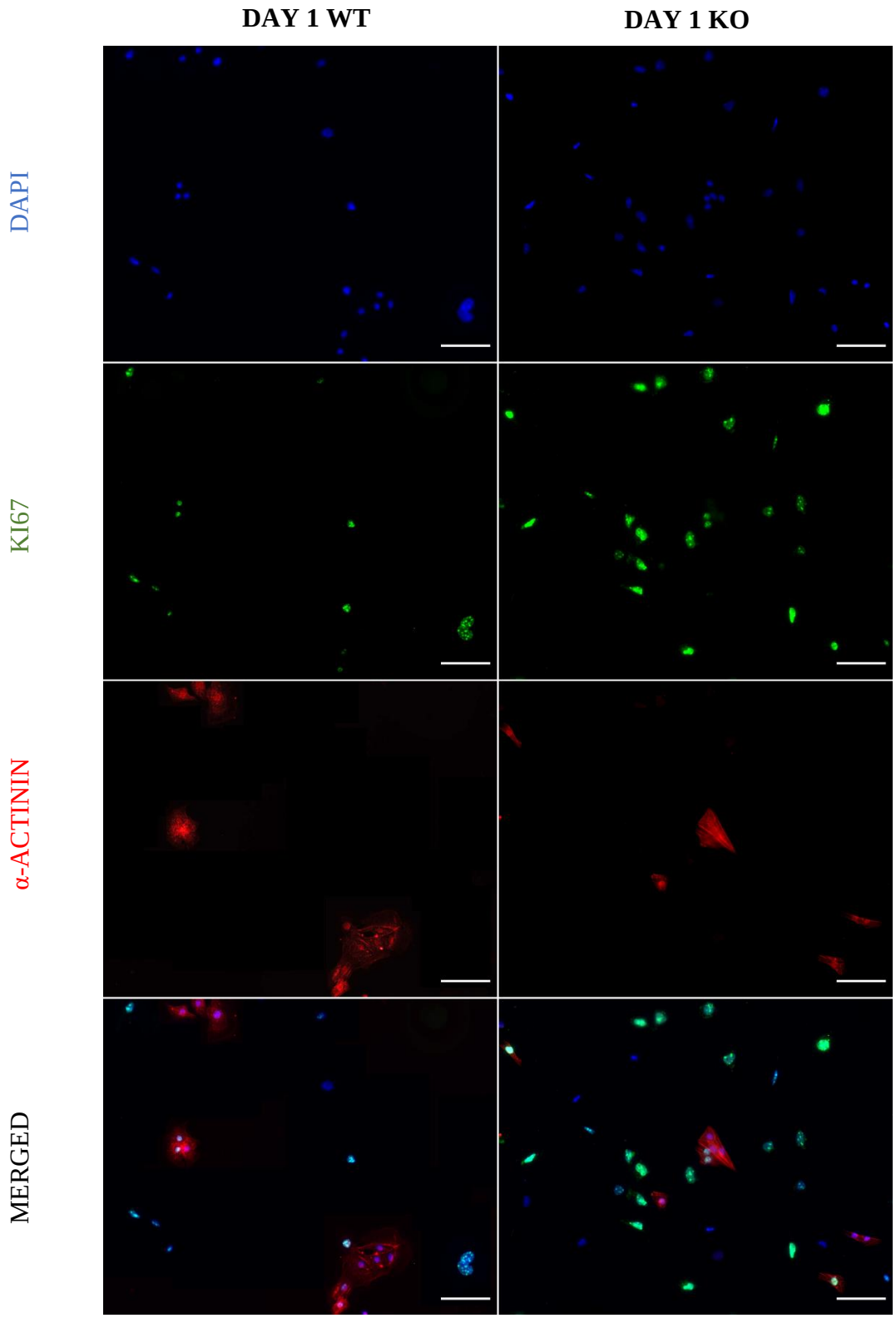

Figure 8: E13 WT and *Cerl2* KO cardiomyocytes at 1 day of culture Immunofluorescence of cardiomyocytes from E13 WT (top row) and E13 *Cerl2* KO (bottom row) embryos at 1 day in culture**.** Cardiomyocytes represent the α-ACTININ^{+} cells and the proliferating cells are KI67^{+}. Bar, 100µm.

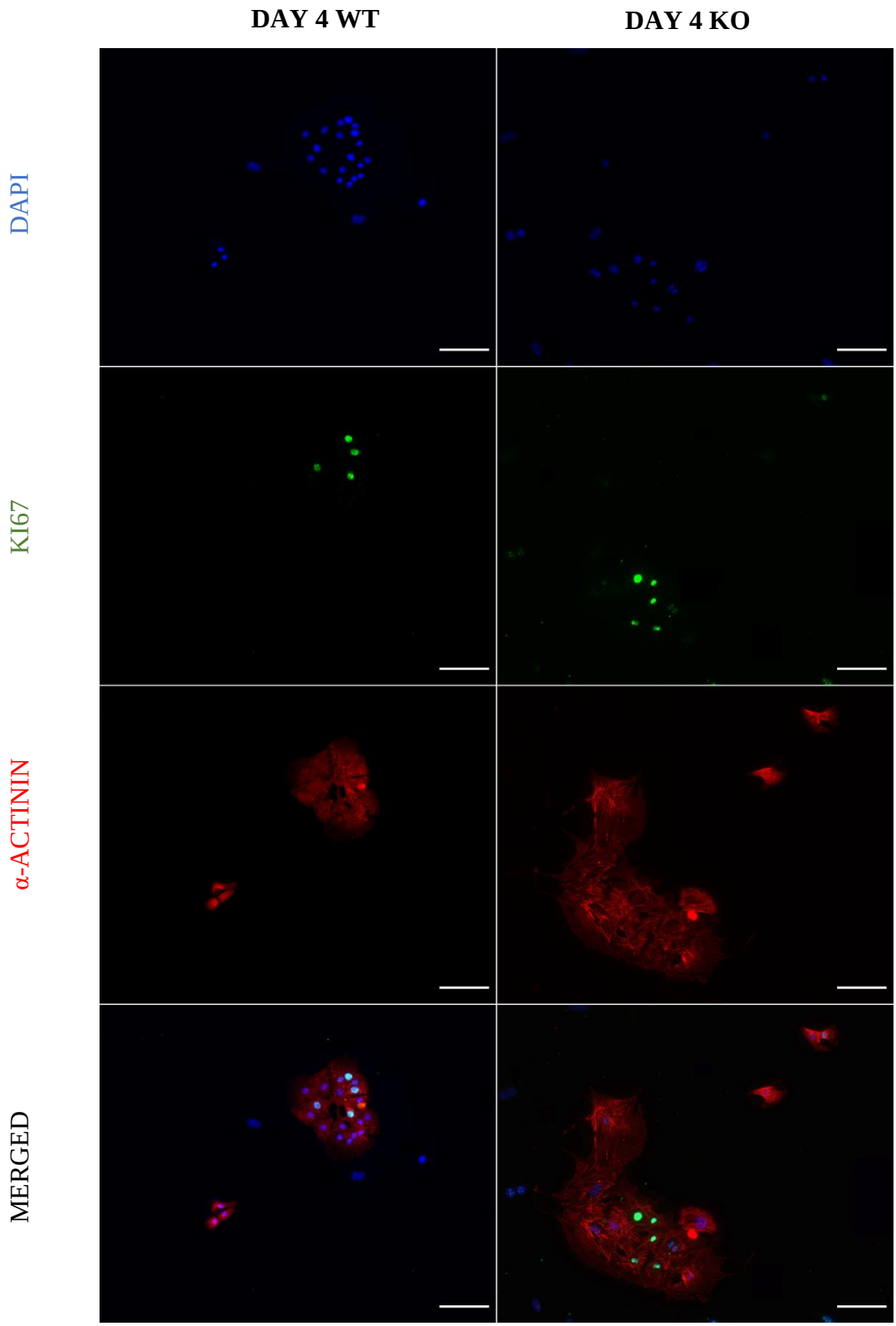

Figure 9: E13 WT and *Cerl2* KO cardiomyocytes at 4 days of culture Immunofluorescence of cardiomyocytes from E13 WT (top row) and E13 Cerl2 KO (bottom row) embryos at 4 days in culture**.** Cardiomyocytes represent the α-ACTININ^{+} cells and the proliferating cells are KI67^{+}. Bar, 100µm.

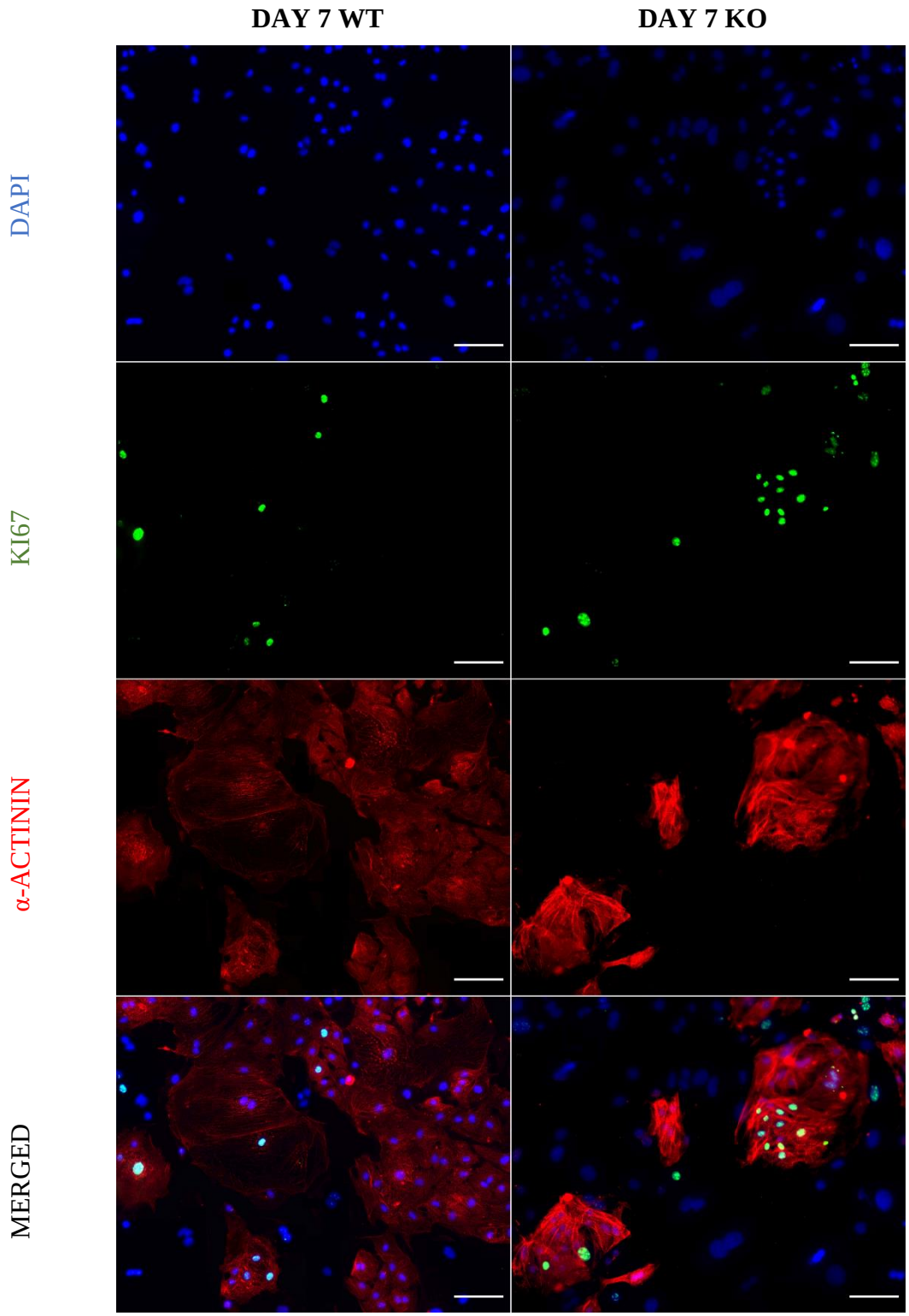

Figure 10: E13 WT and *Cerl2* KO cardiomyocytes at 7 days of culture Immunofluorescence of cardiomyocytes from E13 WT (top row) and E13 *Cerl2* KO (bottom row) embryos at 7 days in culture**.** Cardiomyocytes represent the α-ACTININ^{+} cells and the proliferating cells are KI67^{+}. Bar, 100µm.

Our results show that on all three days of culture, *Cerl2* KO cardiomyocytes have a higher proliferation rate when compared to WT (Figure 11).

On day 1 these percentages are significantly different with a p-value of 0.0161 (p-value<0.05) and a difference between means of 14.50 ± 4.311%. In this day we observed the highest and the lowest proliferation percentage of all days: 40% for *Cerl2* KO and 13% for WT. Average proliferation for *Cerl2* KO was 34% against 19% from WT.

WT cardiomyocytes show an increase in proliferation at day 4. Increasing to an average of 19% to 27%. *Cerl2* KO cardiomyocytes, however, increase to 36% on average. They are still proliferating more with a difference between means of 8.750 ± 2.735%. The results are still significantly different with a p-value of 0.0219 (p-value<0.05).

Day 7 shows a decrease of proliferation for WT cardiomyocytes, closer to the day 1 results on average – 19%, while *Cerl2* KO only show a slight decrease – 33%. The differences between both were the most significantly different with a p-value of 0.0036 and a difference between means of 14.25 ± 3.295%.

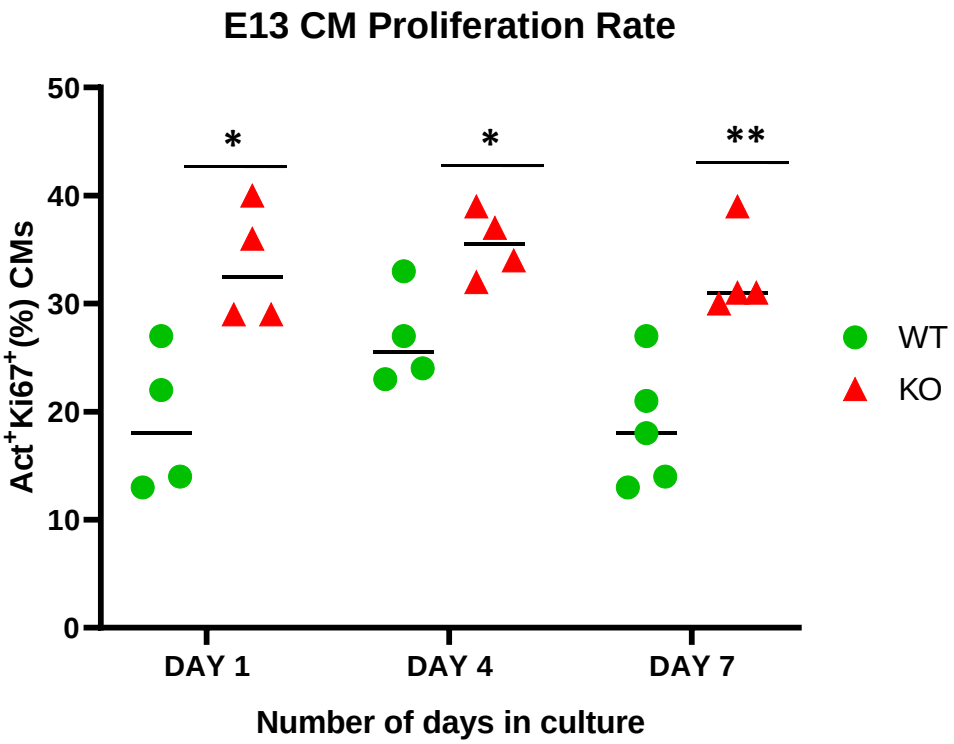

Figure 11: E13 Proliferation Rate Analysis. The figure shows the percentage of proliferating cardiomyocytes (Act^+Ki67^+) from E13 *Cerl2* KO (red) and E13 WT embryos (green) at 1, 4 and 7 days in culture. WT E13 cardiomyocytes (green) are proliferating less on average than the *Cerl2* KO E13 (red) at every day of culture. Day 1 and Day 4 show significant differences with difference between means (SEM) of 14.50% and 8.75%, respectively. In Day 7 the difference between the WT and *Cerl2* KO cardiomyocytes is the biggest with a SEM of 14.15%. n = 4 per group. The top black bar represents the median values. Data was statistically significant when P<0.05 (*). **P<0.01

Altogether, the results indicate that *Cerl2* KO cardiomyocytes isolated at E13 have a higher proliferation rate *in vitro* and can maintain it for at least 7 days in culture. These results are in accordance with previous findings in the developing heart.

4.4 Isolation of the E15 cardiomyocytes

After the E13 experiment was finished, we followed the same optimized steps for the E15 protocol. We removed the ventricles of E15 embryos and placed them in the same collagenase solution. However, E15 hearts are much bigger and developed than the E13 ones, having higher numbers of fibroblasts and therefore more collagen bonds to break. This led to some difficulties in making sure the cardiomyocytes were well isolated. We eventually had to double the time the cells spent in the collagenase solution and increase the number of times we did the mechanical disaggregation of the cells. 7 pregnant females were used at this stage. 4 of the females were KO and the other 3 were WT. In total, we ended up with 12 and 18 embryos respectively. After neutralizing the collagenase solution, cell numbers were also counted in the Neubauer chamber. Number of cells per heart were around 250,000-300,000 on average. They were also placed in 24 well plates coated with gelatin and divided for three different time points – 1, 4 and 7 days after culture.

4.5 Analysis of the E15 cardiomyocytes

Before we tested the proliferation rate of these E15 cardiomyocytes, it was important again to observe and analyze the cell cultures. For this we used immunofluorescence assays, using the same markers that were experimented for the E13 culture (Figures 12, 13 and 15). We found cardiomyocytes that stained for α-actinin and again non-cardiomyocytes that were α-Act$^-$.

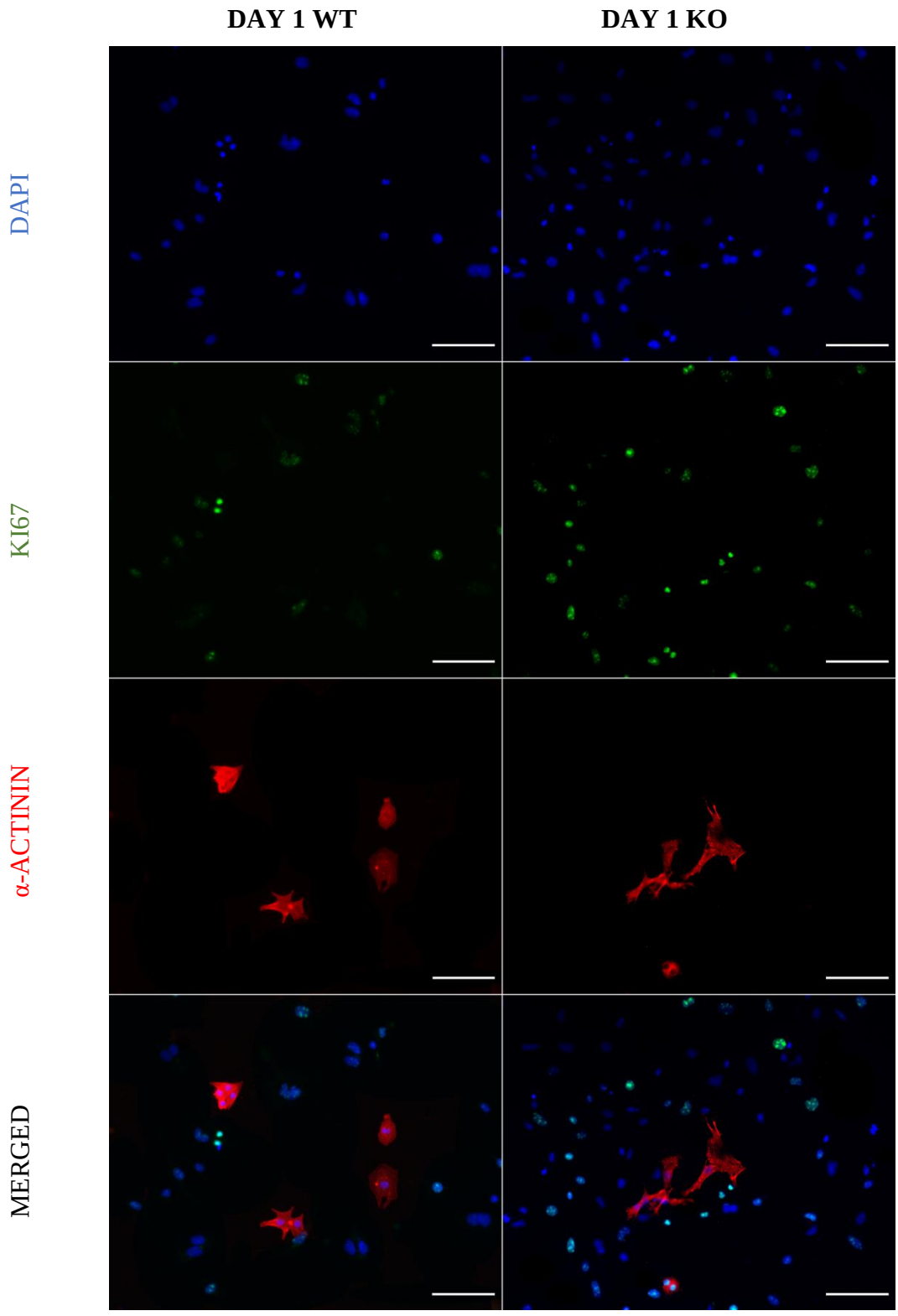

Figure 12: E15 WT and *Cerl2* KO cardiomyocytes at 1 day of culture Immunofluorescence of cardiomyocytes from E15 WT (top row) and E15 *Cerl2* KO (bottom row) embryos at 1 day in culture**.** Cardiomyocytes represent the α-ACTININ^{+} cells and the proliferating cells are KI67^{+}. Bar, 100µm.

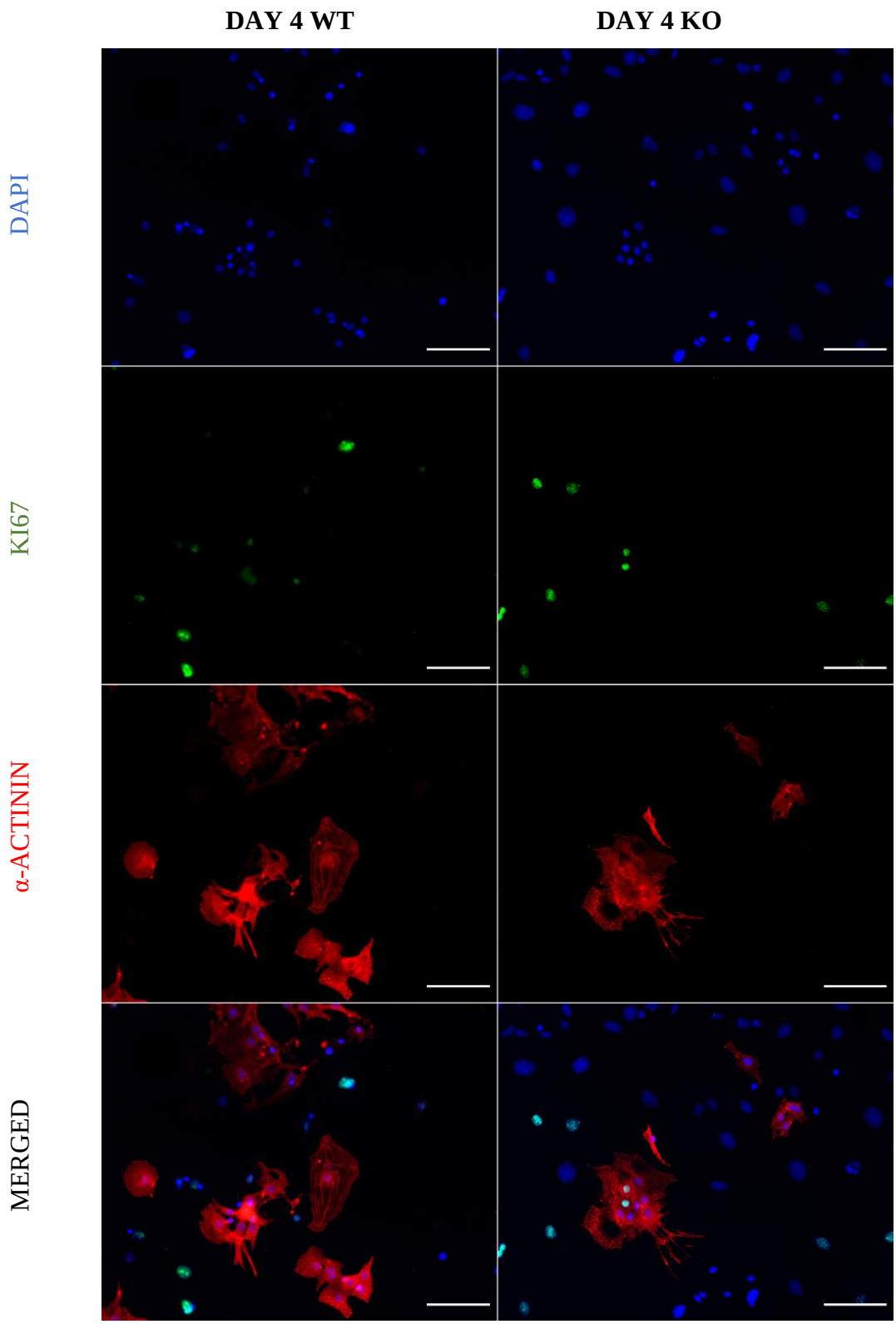

Figure 13: E15 WT and *Cerl2* KO cardiomyocytes at 4 days of culture Immunofluorescence of cardiomyocytes from E15 WT (top row) and E15 *Cerl2* KO (bottom row) embryos at 4 days in culture**.** Cardiomyocytes represent the α-ACTININ^{+} cells and the proliferating cells are KI67^{+}. Bar, 100µm.

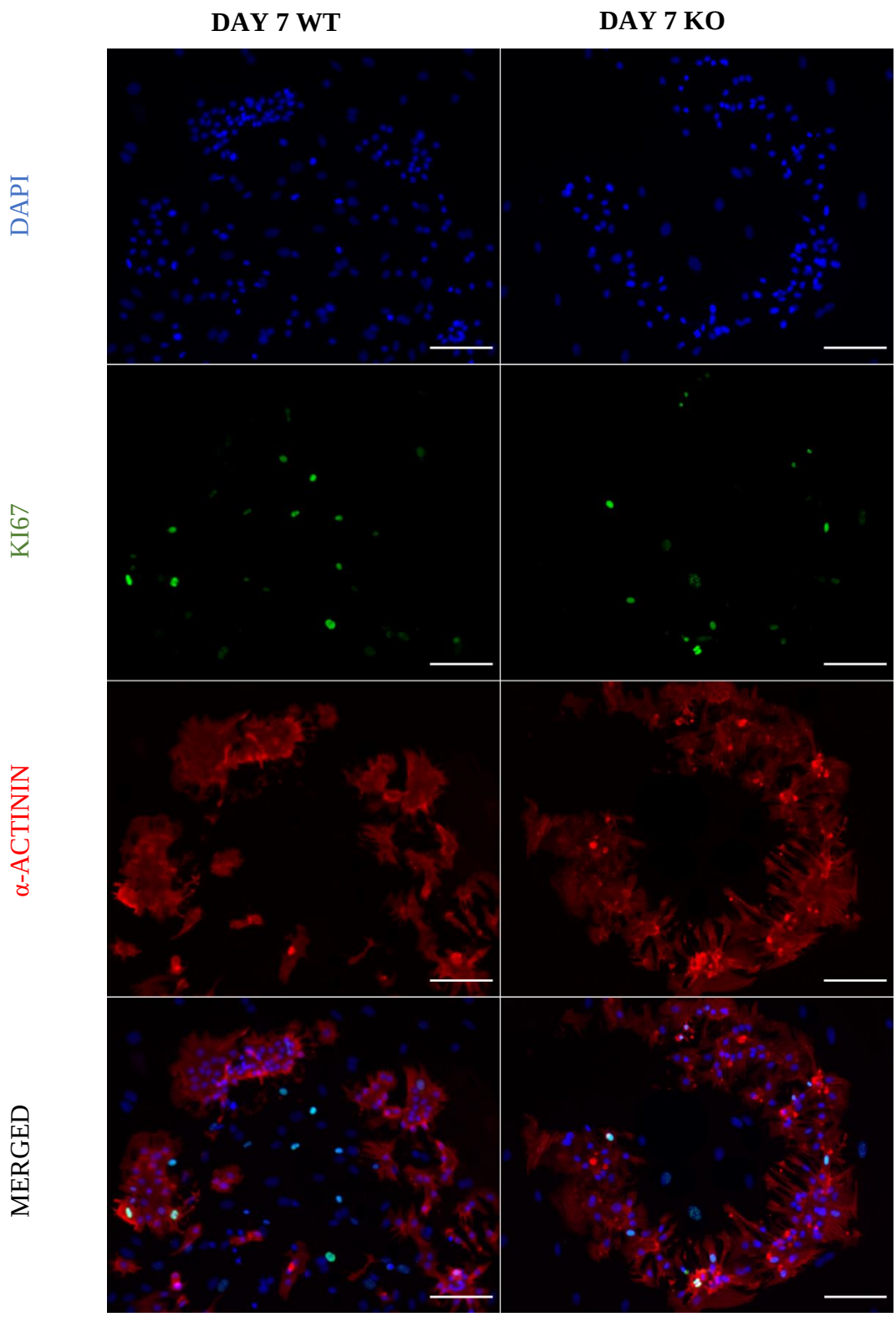

Figure 14: E15 WT and *Cerl2* KO cardiomyocytes at 7 days of culture Immunofluorescence of cardiomyocytes from E15 WT (top row) and E15 Cerl2 KO (bottom row) embryos at 7 days in culture**.** Cardiomyocytes represent the α-ACTININ^{+} cells and the proliferating cells are KI67^{+}. Bar, 100µm.

4.6 E15 *Cerl2* KO cardiomyocyte proliferation rate is significantly different from WT at Day 1

The same study that showed an increase in the mitotic index of the E13 *Cerl2* KO cardiomyocytes of the myocardium wall, has also showed that there was an increase at E15. However, this increase was much lower than at E13 and P0 and therefore not statistically significant. We found that since we had confirmed the result for E13 *in vitro*, it was important to see if the proliferation at E15 *in vitro* was also lower.

Our results show that E15 *Cerl2* KO cardiomyocytes have a significantly higher proliferation rate when compared to WT only on day 1 after culture (Figure 15). The rest of the days have similar proliferation percentages.

On day 1 these percentages are highly significantly different with a p-value of 0.0005 (p-value<0.05) and a difference between means of 9,458 ± 2,229%.

WT cardiomyocytes show an increase in proliferation at day 4. Increasing to an average of 9,25% to 16%. *Cerl2* KO are proliferating slightly more with a difference between means of 0,8750 ± 3,832%. However, the results are not significantly different with a p-value of 0.8230 (p-value<0.05).

Day 7 shows a decrease of proliferation for WT cardiomyocytes, closer to the day 1 results on average, while *Cerl2* KO only show a slight decrease. The differences between both are not significantly different with a p-value of 0.1320 and a difference between means of 7,625 ± 3,981%.

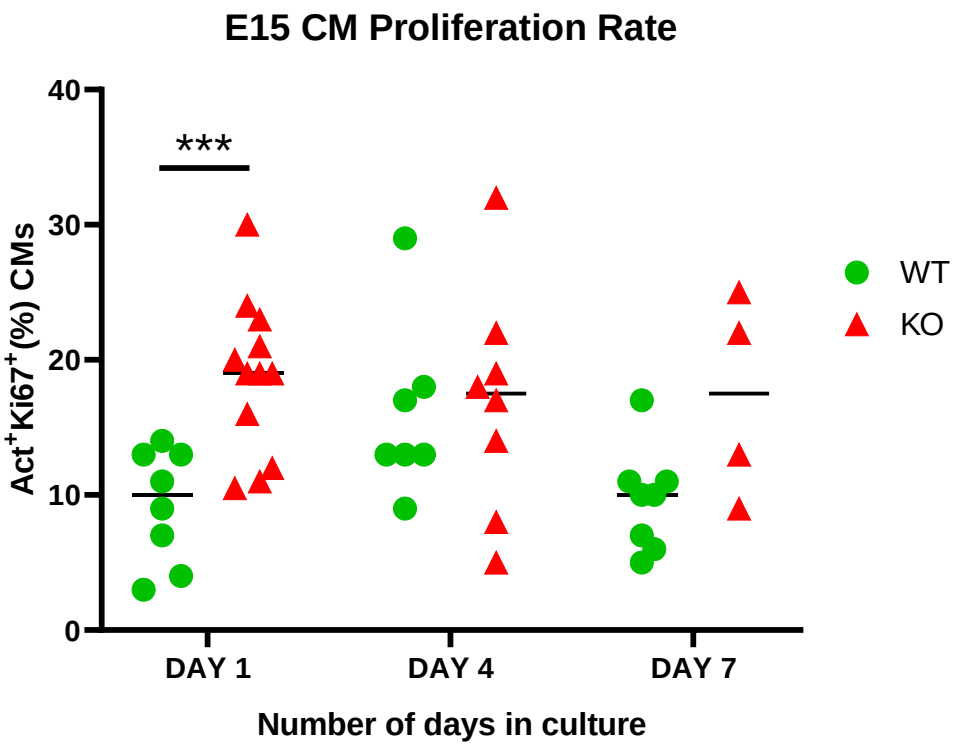

Figure 15: E15 Proliferation Rate Analysis. The figure shows the percentage of proliferating cardiomyocytes ($Act^{+}Ki67^{+}$) from E15 *Cerl2* KO (red) and E15 WT embryos (green) at 1, 4 and 7 days in culture. WT E15 cardiomyocytes proliferate less on average than the *Cerl2* KO E15 (red) at every day of culture. At Day 1 the difference of proliferation between WT and KO cardiomyocytes is substantially significant different with a difference between means (SEM) of 9.46%. In Day 4 and Day 7 the difference between the WT and *Cerl2* KO cardiomyocytes were not statistically significant with a SEM of 0.78% and 7.63%. n = 8 in the WT Day 1 and 4 and n = 7 at Day 7. n = 12 in the *Cerl2* KO Day 1. n = 8 and n = 4 on the *Cerl2* KO Day 4 and *Cerl2* KO Day 7, respectively. The top black bar represents the median values. Data was statistically significant when $P<0.05$ (*). ***$P<0.001$

4.7 Proliferation rates of E13 WT and *Cerl2* KO cardiomyocytes are significantly higher than at E15

Our previous results provided evidence that E13 *Cerl2* KO cardiomyocytes have a higher proliferation rate than WT, while the differences were not significant at E15. We know that cardiomyocyte proliferation during cardiac development involves significant spatial and temporal differences (Hashimoto H. et al, 2014). So, we decided to compare the proliferation differences in these two different embryonic stages in culture. Our results show a decrease in proliferation from E13 to E15. The biggest difference was found at day 4 with a difference between means of 10,75 ± 3,319 (p-value < 0.05). The smallest difference was found at day 7 with a difference between means of 8,975 ± 2,871 (p-value < 0.05). Day 1 showed some differences, half of the E13 cells were proliferating more than the E15. However, overall, they were not significantly different.

These results were as expected for these embryonic stages. In mice, cardiomyocyte proliferation peaks around E10–12 and then decreases until birth (Toyoda M. et al, 2003). A previous study had demonstrated that E12 WT cardiomyocytes increase 120-fold in number while in culture. E15 cardiomyocytes increase 50-fold in number, while E20 only increase 5-fold (Burton P.B.J. et al, 1999).

Therefore, our results are in agreement with these findings, we have also observed *in vitro* that the proliferative capacity of embryonic cardiomyocyte decreases with developmental age (Figure 16).

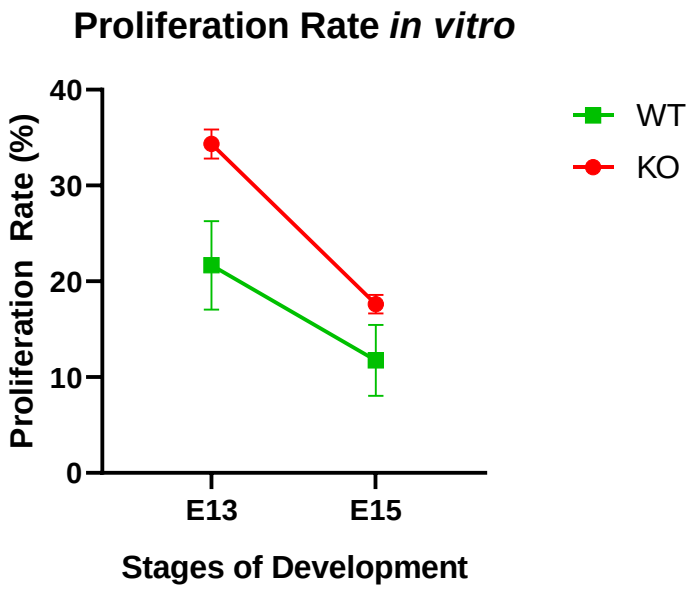

Figure 16: Proliferation Rate *in vitro*. Comparison of the average proliferation rate of Day 1, 4 and 7 in culture of the cardiomyocytes of the E13 and E15 *Cerl2* KO with the E13 and E15 WT. The KO cardiomyocytes (red) proliferate more than the WT in both embryonic stages. The E13 *Cerl2* KO cardiomyocytes have a higher statistically significant proliferation rate than the E13 WT cardiomyocytes. Difference between means (SEM) of 12.67%. The difference is not significative between both types at E15. There is also a decrease in proliferation rate from the E13 to the E15 *Cerl2* KO of 16.72%. In the WT the decrease is only of 9.92. The bar represents the median values. Data is presented as mean ± SEM.

Cerl2 is expressed in the heart until E13. Its absence leads to a higher cardiomyocyte proliferation at E13, but not at E15 in the developing heart (Araújo A. et al, 2014) and *in vitro* as we proved before. WT proliferation rate comparison at E13 and E15 confirmed previous results that cardiomyocytes *in vitro* proliferate less with developmental age at the time of isolation (Figure 18). These different results should also be found in our *Cerl2* KO cells. In fact, our results show a decrease in proliferation from E13 to E15 at all days in culture. The biggest difference was found at day 4 *Cerl2* KO with a difference between means of 18.63 ± 3.339 (p-value < 0.05) (Figure 17). The smallest difference was found at day 7 with a difference between means of 14,79 ± 3,185 (p-value < 0.05). These differences are also higher than the differences between the WT cells. At E13 the difference in proliferation is so significant that it leads to a much thicker myocardium and heart defects at birth. So, it comes to no surprise that the difference in these *Cerl2* KO cells at different time points is higher than in the WT.

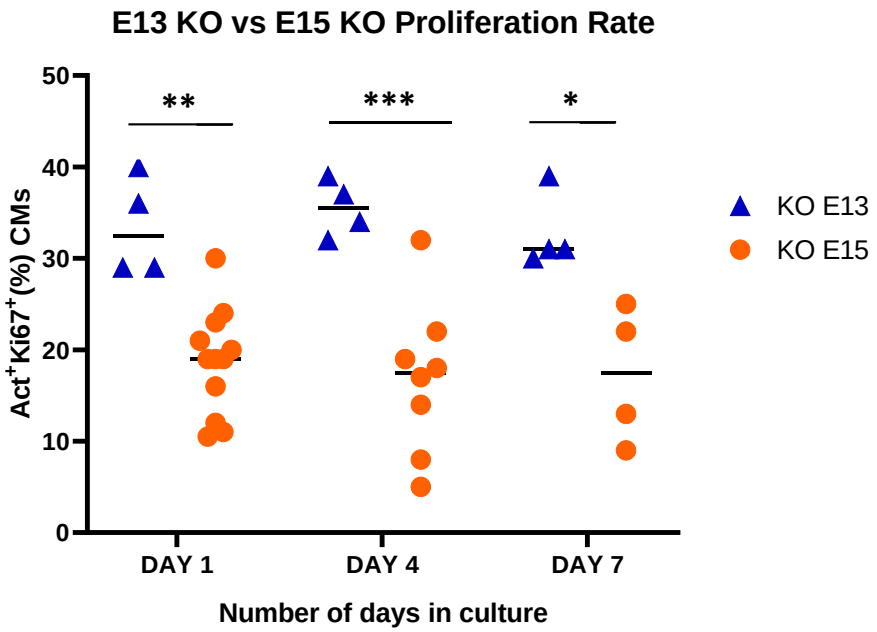

Figure 17: E13 vs E15 KO Proliferation Rate Comparison. The figure shows the percentage of proliferating cardiomyocytes (Act^+Ki67^+) from E13 *Cerl2* KO (blue) compared with E15 *Cerl2* KO embryos (orange) at 1, 4 and 7 days in culture. E13 KO cardiomyocytes proliferate more on average than the E15 *Cerl2* KO at every day of culture. The most significant difference was found on Day 4 with a difference between means (SEM) of 18.63%. The second biggest difference was at Day 1 with a SEM of 14.7% and the smallest at Day 7 with a SEM of 15.50%. n=4 for the E13 *Cerl2* KO group. n = 12 in the E15 *Cerl2* KO Day 1. n = 8 and n = 4 on the E15 *Cerl2* KO Day 4 and *Cerl2* KO Day 7, respectively. The top black bar represents the median values. Data was statistically significant when P<0.05 (*). **P<0.01. ***P<0.001

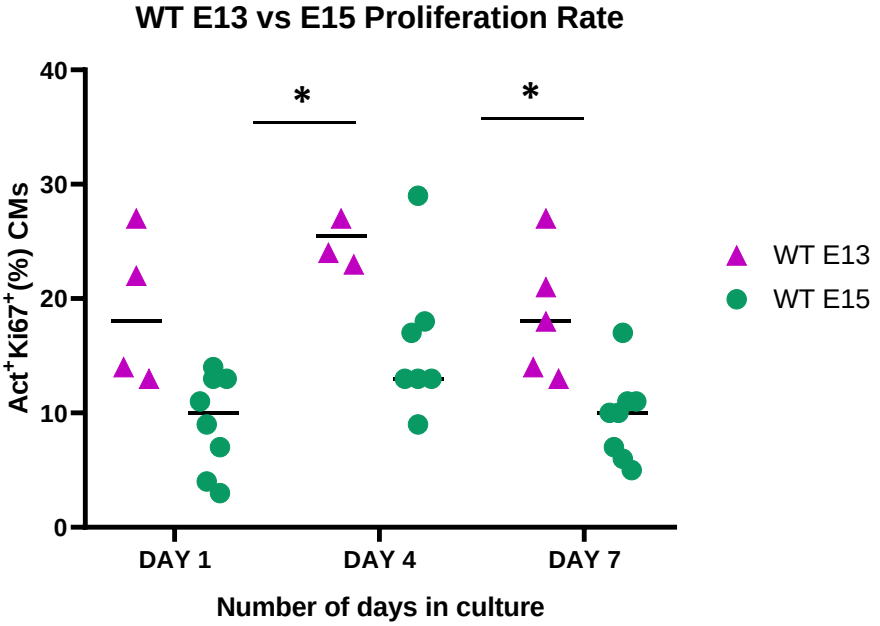

Figure 18: E13 vs E15 WT Proliferation Rate Comparison. The figure shows the percentage of proliferating cardiomyocytes (Act^+Ki67^+) from E13 WT (purple) compared with E15 WT embryos (green) at 1, 4 and 7 days in culture. E13 WT cardiomyocytes proliferate more on average than the E15 WT at every day of culture. Statistically significant differences were found at Day 4 and Day 7 with a difference between means (SEM) of 10.75% and 8.98%. n=4 for the E13WT group. n = 12 in the E15 *Cerl2* KO Day 1. n = 8 in the WT Day 1 and 4 and n = 7 at Day 7. The top black bar represents the median values. Data was statistically significant when P<0.05 (*).

5. Discussion

5.1 Discussing the results

Cardiovascular diseases have been the main cause of morbidity and mortality in developed countries, representing almost 50% of all deaths in Europe (Townsend et al, 2016). Cardiac disease progression often involves cardiac stress resulting in cardiomyocyte death and the formation of non-contractile scar tissue (Coulombe et al., 2014). Unfortunately, adult heart myocardial cells have limited regeneration capacity due to the limited proliferative capacity of cardiomyocytes. Several heart therapies have been developed to minimize the symptoms of heart disease; however, they are non-curative and generally only minimize the symptoms of the disease. Heart transplantation has seen major improvements in patient recovery and well-being, but it is very limited in resources and comes with associated immunosuppression (Moran AE., 2014). Ideally, the use of the patient's PSCs as a source of new cardiac cells to be implanted in the heart, would be a great alternative solution. Despite its many advances, the use of PSCs to derive cardiomyocytes comes with a challenge - the isolation and expansion of large number of cardiomyocytes. Therefore, the study and design of new models looking to increase the capacity of cardiomyocytes to proliferate is fundamental for future regenerative cardiovascular medicine.

Loss-of-function of Cerl2 in mice has been associated with an increase in the mitotic index of the cardiomyocytes of the compact myocardium of the heart ventricular walls (Araújo et al, 2014). This increase is associated with prolonged TGF-β/Nodal and Wnt/β-catenin signaling, signaling pathways known to be antagonized by the Cerberus/Dan family. Both signaling pathways are known to have a role in cardiac proliferation and differentiation, and *Cerl2* is the only known member of this family to be expressed in the heart. So, we propose that Cerl2 functions as a modulator of these pathways and is therefore potential regulator of cardiomyocyte proliferation.

Cardiomyocyte differentiation and proliferation at precise time windows in development is important for proper heart formation. When the cells are subjected to even the smallest shift in the spatial and temporal expression of their signaling pathways, a combined effect of problems can emerge damaging the heart or to a more extent arrest embryo development altogether.

Cerl2 was found to be an important mediator in the L-R axis formation during development. Its capability to bind and block Nodal activity is important for the Nodal asymmetrical expression in the L-LPM that leads to the formation of the first asymmetric organ to be formed, the heart (Marques et al, 2004). Later, Cerl2 was also found to be important in specific stages of heart development. *Cerl2* KO mice are born with several LD defects and most die a few hours after birth due to heart defects. An analysis to the hearts of *Cerl2* KO mice hearts with no LD defects had shown an increase in the compact myocardium of both left and right ventricles. Further results showed an increase in the mitotic index of the cardiomyocytes in the compact myocardium at E13 and P0. This increase is associated with a higher cardiomyocyte proliferation and explains the myocardium thickness by hyperplasia of the cells. At E15 there was a significant decrease in mitotic index between these embryonic stages. Despite still having a higher mitotic index than the WT, it was not considered to be statistically significant. pSmad2 and ß-catenin levels were also found to be elevated in *Cerl2* KO E13 and P0 hearts (Araújo A. et al, 2014).

Since the *Cerl2* KO cardiomyocytes have an increased mitotic index leading to ventricular hypertrophy and this defect seems to be unrelated to laterality defects, it appears that Cerl2 has some cardiomyocyte-

specific roles (Araújo A. et al, 2014). Determining which signaling pathways are deregulated in the *Cerl2* KO cardiomyocytes leading to increased proliferation is important for providing us with the basis to try and manipulate the proliferation isolated cardiomyocytes. Therefore, it is important to assess if the same differences in proliferation are also found *in vitro*, followed by supplementing small molecule activators/inhibitors of TGF-β/Nodal and of Wnt/β-catenin signaling to the isolated WT and *Cerl2* KO cardiomyocytes and evaluate their effect on the proliferation rate.

To assess how the *Cerl2* KO cardiomyocytes proliferated *in vitro*, we decided to isolate the cardiomyocytes of E13 and E15 WT and *Cerl2* KO hearts, since they were two of the stages previously studied. We started by isolating and analyzing the E13 cells. Our results show that there is a significant difference between the E13 *Cerl2* KO cardiomyocyte proliferation rate and the WT proliferation rate. As mentioned before, there is a pick of proliferation at E13-E13-25 associated with a higher mitotic index in the *Cerl2* KO heart. At 1 day after culture of the E13 *Cerl2* KO cells we can still see a higher proliferation rate, as expected. However, WT has a much lower value. Fetal cardiomyocytes in culture usually have lower proliferation rates. A study at E12 has reported an average of 7% of cells reaching the S phase *in vitro*, with a maximum value of 15% in a cardiomyocyte enriched culture (Rodgers, L.S., et al., 2009). Another study at E14.5 with a normal culture has demonstrated that only 21.15% of WT cardiomyocytes reach the S phase and 13.85% reach G2/M stage (Walsh S. et al, 2010). The difference in proliferation for the E13 *Cerl2* KO declines after 4 days but is still significantly higher than in the WT cells and will continue to be for the remaining days. This higher proliferation rate agrees with previous results (Araújo A. et al, 2014). pSMAD2 levels of *Cerl2*$^{-/-}$ KO hearts were reported to be higher and appear to continue until neonatal stage. This could mean that the same levels kept being higher in culture and had a prolongated effect. This would result in an increase in TGF-ß /Nodal signaling that is involved in cell proliferation.

ß-catenin levels were also reported to be high at E13. Wnts represent highly conserved secreted glycoproteins that trigger receptor-mediated signal transduction cascades (Garriock, R.J. et al, 2007). Upon binding to the receptor, Wnts can activate various outputs in a β-catenin-dependent (canonical response) or β-catenin-independent (non-canonical response) manner (Działo, E. et al, 2018). In the canonical response, Wnts prevent degradation of β-catenin by inhibition of glycogen synthase kinase 3β (GSK3β)-dependent degradation complex. β-catenin is then translocated into the nucleus, where it activates T-cell factor (TCF)/lymphoid enhancer factor (LEF) and regulates expression of Wnt/β-catenin target genes like Cyclin D2 that promote cell proliferation (Valenta, T. et al, 2012). Wnt/β-catenin signaling pathway also controls spatiotemporal proliferation and differentiation of early ventricular myocytes derived from mouse fetal ventricular myocytes (Buikema et al., 2013). Furthermore, constitutively activated β-catenin in fetal ventricular myocardium promotes proliferation of cardiomyocytes in the left and right ventricle up to the early neonatal stage. β-catenin reduced signaling attenuates proliferation of early ventricular myocytes and differentiation mainly in the compact myocardium (Buikema et al., 2013). Direct inhibition of GSK3β, which activates Wnt/β-catenin signaling, was found to enhance the *in vitro* proliferation capacity of early cardiomyocytes. Furthermore, a TGF-β pathway was reported to inhibit GSK-3β. Thus, TGF-β might directly activate the β-catenin-dependent pathway through direct deactivation of GSK-3β (Ma et al., 2017). Activated Wnt/β-catenin, in turn, stabilizes the TGF-β/Smad response since the Smad/β-catenin/Lef protein complex regulates a host of shared target genes, often in a synergistic manner (Xing Guo & Xiao-Fan Wang, 2009).

Therefore, we propose that *in vitro*, since Cerl2 is absent in the *Cerl2* KO embryo heart at this critical stage, and because *in vitro* there is the absence of other cell signals from the heart that could inactivate

it, ß-catenin is still being produced, Wnt/ß-catenin signaling is active, leading to the *Cerl2* KO cardiomyocytes proliferation at higher percentages.

Our results at E15 *in vitro* were also in agreement to the *in vivo* observations that there is an overall decrease in the proliferation rates of E15 cardiomyocytes (Araújo et al, 2014). We found that despite being lower compared to E13, E15 *Cerl2* KO cardiomyocyte proliferation was significantly different than the WT at day 1. The following days showed some differences, but not significant. The differences observed at day 1 could be explained by the remaining effects of the Cerl2 inhibition in the Wnt/ß-catenin and the TGF-ß signaling pathways. However, these effects seem to not be sufficient to maintain a higher proliferative state in the following days of culture. At this stage in development, it is expected that the Wnt/ß-catenin and the TGF-ß signaling pathways are already being downregulated by other inhibitors. In fact, there is an overall decrease in proliferation at this developmental stage in the normal developing heart. Both WT and *Cerl2* KO E15 show a decrease *in vivo* and *in vitro*, so we can assume that Cerl2 no longer plays a role in this stage of development.

Altogether, our results show that Cerl2 is not only capable of regulating cardiomyocyte proliferation *in vivo*, but also *in vitro*. Its absence in the heart is most prominent at E13, where the differences in proliferation between *Cerl2* KO and WT cardiomyocytes are the most significative. Cerl2 should therefore be considered as potential regulator in cardiac proliferation (Figure 19).

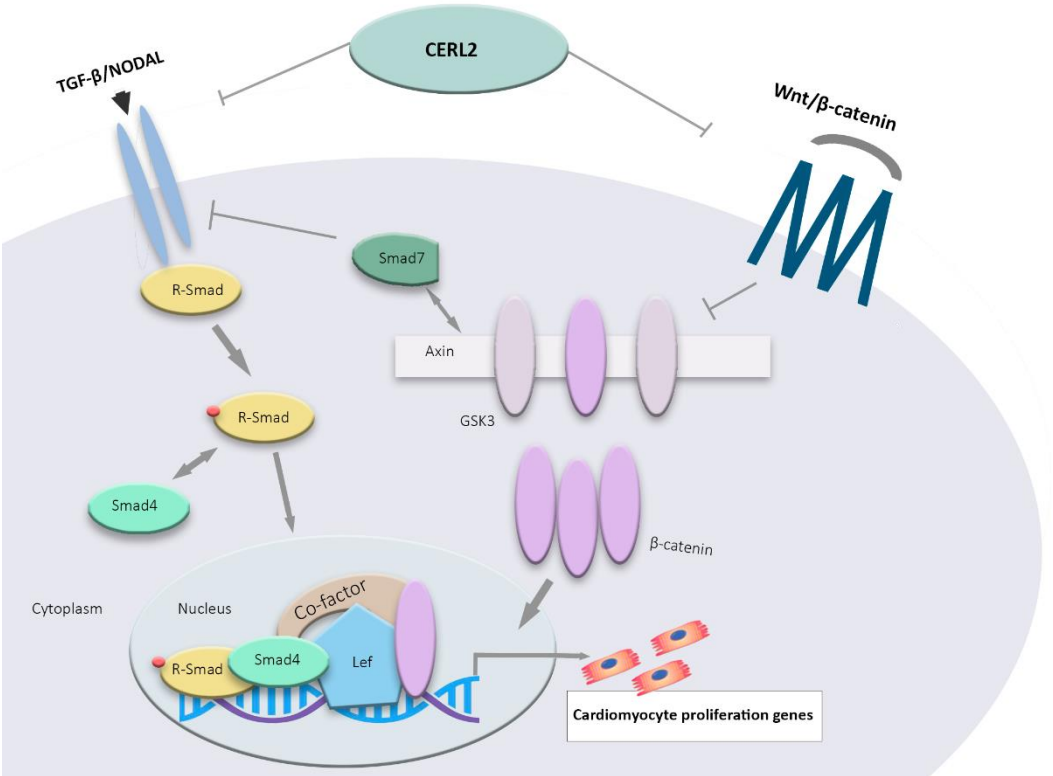

Figure 19: Cerl2 interaction with cardiomyocyte proliferation signaling pathways. Cerl2 inhibits TGF-β/Nodal and/or Wnt/β-catenin leading to the higher expression of Smads and β-catenin, respectively. These activate genes in the nucleus related to cardiomyocyte proliferation genes. (Adapted from Xing Guo et al, 2009).

5.2 Future Perspectives

In the future, an immunofluorescence assay should be performed to confirm the presence of higher levels of the Wnt/ß-catenin and TGF-ß signaling pathways. Western blotting should be performed to further validate the results. Also, since E13 *Cerl2* KO mice proliferate more, it would be interesting to rescue its expression *in vitro* by adding exogenous Cerl2 to the culture and measuring the resulting proliferation rate. This also could be done with TGF-ß/Nodal and Wnt/ß-catenin inhibitors to compensate for the lack of inhibition of the Cerl2 protein.

The proliferation rates for the E13 and E15 mice were only verified through immunofluorescence. An immunofluorescence assay has some important variables to take in consideration. Despite using the same protocols and conditions, such as: antibody concentration and timing during protocol execution; and the same time exposure during microscope photography; Ki67 staining is not always as strong in all nuclei. Therefore, cell counting in immunofluorescence is not exact. This could be because of different phases and levels of the protein present in the nucleus of the cell as well as some user error while performing the protocol. Therefore, fluorescence-activated cell sorting (FACS) should be considered in the future to further validate these results. Also, Ki67 is present in several phases of the cell cycle and it is not possible to distinguish them without other markers, such as Bromodeoxyuridine (BrdU). BrdU is a synthetic thymidine analog that incorporates into cell DNA at its replication phase of the cell cycle – phase S. Phosphohistone H3 (PHH3) is a core histone protein that is present in the chromatin in eukaryotic cells. PHH3 levels are negligible during interphase but reach a maximum for chromatin condensation during mitosis, making it a good phase M marker. A BrdU incorporation assay with a DNA marker, such as 7-AAD, together with a PHH3 assay should be able to separate the populations by the different cell cycle phases G0/G1, S, and G2/M using FACS. These results would also give us insights regarding the *in vitro Cerl2* KO cardiomyocytes having a higher mitotic index and a higher number of cells at day 7 than the WT.

Results showed that non-cardiomyocyte cell proliferation had no differences between E13 *Cerl2* KO, and WT. However, we found a slightly bigger percentage of these cells in the *Cerl2* KO culture. So, it would be expected to see a little more non-cardiomyocyte cell proliferation. But since those results were not significantly different, it was probably a result of user error or the pictures chosen for counting having by chance more non-cardiomyocyte cells than cardiomyocytes. A FACS assay would be a more accurate assay to measure correctly all the α-Act$^+$ and vimentin$^+$ in culture. The presence of higher percentages of non-cardiomyocytes in culture has been shown to improve the cardiomyocytes proliferation. As such, it would be interesting to see how they affected the *Cerl2* KO proliferation *in vitro*. Also, as mentioned before, vimentin is the major intermediate filament found in non-muscle cells (Colvin et al., 1996). Non-muscle cells include fibroblasts, endothelial cells, macrophages, melanocytes, Schwann cells, and lymphocytes. At E13 we expect to find several types of cells, such as: cardiomyocytes and endothelial cells derived from mesodermal cells; cardiac fibroblasts and smooth muscle cells from the proepicardium. Therefore, it is possible that the vimentin$^+$ cells are not only cardiac fibroblasts but also endothelial-type cells. In the future Discoidin Domain Receptor 2 (DDR2) should be used to confirm and distinguish the type of cells found at this stage. DDR2 is a collagen receptor and is therefore a fibroblast-specific marker (Baudino et al., 2006; Camelliti et al., 2005; Goldsmith et al., 2004), and a previous study has showed that it does not stain endothelial or smooth muscle cells in the heart at E12.5 (Ieda M., et al., 2009).

Another aspect we should have in consideration for this study is the probability of cardiomyocytes becoming binucleated in culture. Cardiomyocytes in the developing heart and at the one-day old

neonatal mouse are predominantly mononucleated with percentages varying between different studies and techniques. In these stages there is a lower content of sarcomeres, but myofibrils still need to disassemble before cell division (Ahuja P. et al, 2004). This disassembly is a sign of dedifferentiation usually accompanied by proliferation and is vital for cell cycle completion. However, just 8–9 days after birth, more than 98% of mouse cardiomyocytes become binucleated while losing their proliferative capacity at the same time (Walsh S. et al, 2010). This could be a result of insufficient myofibril disassembly because of the sarcomere maturation that leads to a failure in cytokinesis (Engel FB. et al, 2006). Cardiomyocytes in culture can also become binucleated. The fetal cardiomyocytes spatial arrangement and connections *in vitro* are not the same as in the heart. A study has reported that 5% of E14.5 cardiomyocytes become binucleated 24 hours after culture. This contrasts with the 1% found in tissue (Takeda K. et al, 2003). Most of the cardiomyocytes in day 1 were isolated and with a single nucleus but we could still find double nuclei that were still sharing the same cytoplasm during division. In the later days, cells became closer to each other and started overlapping. Therefore, we cannot guarantee they did not become binucleated. Binucleation happens when cardiomyocytes fail to enter cytokinesis due to incomplete sarcomere disassembly. If in the future binucleation could be confirmed, it would mean that *in vitro* cells tend to grow by hypertrophy instead of hyperplasia, like it was previously shown in heart sections (Araújo A. et al, 2014).

Congenital Heart Defects (CHD) are the main cause of heart defects. 30% of prenatal loss is due to these conditions. Understanding the causes and the pathways involved in these diseases can help us prevent future losses. Also, in the adult heart cardiomyocyte proliferation is unable to contribute significantly to the regeneration of the myocardium. Cardiovascular diseases such as angina and myocardial infarction are the number one cause of death in all continents, but Africa. Our results show that our mutant cardiomyocytes proliferate more than the average. Therefore, they can be used in future regenerative studies of the heart *in vitro* that require significant amounts of cells for testing.

6. References

Ahuja P, Perriard E, Perriard JC, Ehler E. (2004). Sequential myofbrillar breakdown accompanies mitotic division of mammalian cardiomyocytes. J Cell Sci.117:3295–3306.

Araújo, A. C., Marques, S., & Belo, J. A. (2014). Targeted inactivation of cerberus like-2 leads to left ventricular cardiac hyperplasia and systolic dysfunction in the mouse. PLoS ONE, 9(7), 1-12.

Arceci RJ, King AA, Simon MC, Orkin SH,Wilson DB. (1993). Mouse GATA-4: A retinoic acid-inducible GATA-binding transcription factor expressed in endodermally derived tissues and heart. Mol Cell Biol 13: 2235–2246.

Baudino TA, Carver W, Giles W, Borg TK. (2006). Cardiac fibroblasts: friend or foe? Am J Physiol Heart Circ Physiol. 291:H1015–1026.

Beddington, R.S., Robertson, E.J. (1999). Axis development and early asymmetry in mammals. Cell 96, 195–209

Beddington, R.S.P., Robertson, E.J. (1998). Anterior patterning in mouse. Trends Genet. 14, 277–284.

Belo, J. A., Marques, S., & Inácio, J. M. (2017). The Role of Cerl2 in the Establishment of Left-Right Asymmetries during Axis Formation and Heart Development. American journal of cardiovascular disease, 4(4).

Belo, J.A., Bouwmeester, T., Leyns, L., Kertesz, N., Gallo, M., Follettie, M., De Robertis, E.M. (1997). Cerberus-like is a secreted factor with neutralizing activity expressed in the anterior primitive endoderm of the mouse gastrula. Mech. Dev. 68, 45–57.

Belo, J.A., Silva, A.C., Borges, A.-C., Filipe, M., Bento, M., Gonçalves, L., Vitorino, M., Salgueiro, A.-M., Texeira, V., Tavares, A.T., Marques, S. (2009). Generating asymmetries in the early vertebrate embryo: the role of the Cerberus-like family. Int. J. Dev. Biol. 53, 1399–1407.

Ben-Shachar, G., Arcilla, R.A., Lucas, R. V, Manasek, F.J., 1985. Ventricular trabeculations in the chick embryo heart and their contribution to ventricular and muscular septal development. Circ. Res. 57, 759–766.

Bouwmeester, T., Kim, S.-H., Sasai, Y., Lu, B., De Robertis, E.M. (1996). Cerberus is a headinducing secreted factor expressed in the anterior endoderm of Spemann's organizer. Nature 382, 595–601.

Brade, T., Pane, L. S., Moretti, A., Chien, K. R., & Laugwitz, K. L. (2013). Embryonic heart progenitors and cardiogenesis. Cold Spring Harbor perspectives in medicine, 3(10), a013847.

Bruneau B.G. (2008) The developmental genetics of congenital heart disease. Nature. 451:943–948.

Buckingham, M., Meilhac, S., Zaffran, S. (2005). Building the mammalian heart from two sources of myocardial cells. Nat. Rev. Genet. 6, 826–835.

Buikema, J. W., Zwetsloot, P. P., Doevendans, P. A., Sluijter, J. P., & Domian, I. J. (2013). Expanding mouse ventricular cardiomyocytes through GSK-3 inhibition. *Current protocols in cell biology*, *61*, 23.9.1–23.9.10.

Buikema, J.W., Mady, A.S., Mittal, N. V, Atmanli, A., Caron, L., Doevendans, P.A., Sluijter, J.P.G., Domian, I.J. (2013). Wnt/β-catenin signaling directs the regional expansion of first and second heart field-derived ventricular cardiomyocytes. Development 140, 1–12.

C.S. Simon, A.K. Hadjantonakis, C. Schröter (2018). Making lineage decisions with biological noise: lessons from the early mouse embryo. Wiley Interdiscip. Rev. Dev. Biol, 7, p. e319

Camelliti P, Borg TK, Kohl P. (2005). Structural and functional characterization of cardiac fibroblasts. Cardiovasc Res. 65:40–51.

Chen T. Epicardial induction of fetal cardiomyocyte proliferation via a retinoic acid-inducible trophic factor (2002). Dev. Biol. 250(1):198–207.

Colvin, J., Bohne, B., Harding, G. et al. (1996). Skeletal overgrowth and deafness in mice lacking fibroblast growth factor receptor 3. Nat Genet 12, 390–397.

Coulombe, K. L. K., Bajpai, V. K., Andreadis, S. T., & Murry, C. E. (2014). Heart regeneration with engineered myocardial tissue. Annual Review of Biomedical Engineering, 16, 1–28.

Cristo, F., Inácio, J. M., de Almeida, S., Mendes, P., Martins, D. S., Maio, J., Anjos, R., & Belo, J. A. (2017). Functional study of DAND5 variant in patients with Congenital Heart Disease and laterality defects. BMC Medical Genetics, 18(1), 1-9.

Davidson, B.P., Tam, P.P.L. (2000). The node of the mouse embryo. Curr. Biol. 10, R617–R619.

Deng, H., Xia, H., & Deng, S. (2015). Genetic basis of human left-right asymmetry disorders. Expert Rev Mol Med, 16, e19.

Działo, E.; Tkacz, K.; Błyszczuk, P. (2018) Crosstalk between TGF-β and WNT signalling pathways during cardiac fibrogenesis. Acta Biochim. Pol. 2018, 65, 341–349.

Engel FB, Schebesta M, Keating MT. (2006) Anillin localization defect in cardiomyocyte binucleation. J Mol Cell Cardiol. 41:601–612.

F.L. Conlon, K.M. Lyons, N. Takaesu, K.S. Barth, A. Kispert, B. Herrmann, E.J. Robertson (1994). Development 120: 1919-1928;

G. Guo, M. Huss, et al., P. Robson (2010). Resolution of cell fate decisions revealed by single-cell gene expression analysis from zygote to blastocyst. Dev. Cell, 18 (2010), pp. 675-685

Garriock, R.J.; Warkman, A.S.; Meadows, S.M.; D'Agostino, S.; Krieg, P.A. (2005). Census of vertebrate Wnt genes: Isolation and developmental expression of Xenopus Wnt2, Wnt3, Wnt9a, Wnt9b, Wnt10a, and Wnt16. Dev. Dyn. 236, 1249–1258.

Gerard J. Tortora; Berdell R. Funke; Cristine L. Case (2007). Microbiology: an introduction. Pearson Benjamin Cummings. ISBN 0-321-39603-0.

Gessert S, Kuhl M. (2010). The multiple phases and faces of wnt signaling during cardiac differentiation and development. Circ Res 107: 186–199.

Glinka, A., Wu, W., Delius, H., Monaghan, A. P., Blumenstock, C., & Niehrs, C. (1998). Dickkopf-1 is a member of a new family of secreted proteins and functions in head induction. Nature, 391(6665), 357–362.

Goldsmith EC, Hoffman A, Morales MO, Potts JD, Price RL, McFadden A, Rice M, Borg TK. (2004). Organization of fibroblasts in the heart. Dev Dyn. 230:787–794.

Guo, X., & Wang, X. F. (2009). Signaling cross-talk between TGF-beta/BMP and other pathways. Cell research, 19(1), 71–88.

Hall, J. E., & Guyton, A. C. (2011). Guyton and Hall textbook of medical physiology. Philadelphia, PA: Saunders Elsevier.

Hamada, H. (2008). Breakthroughs and future challenges in left–right patterning. Development, Growth & Differentiation, 50: S71-S78.

Hamada, H., Meno, C., Watanabe, D., & Saijoh, Y. (2002). Establishment of vertebrate left–right asymmetry. Nature Reviews Genetics, 3(2), 103–113.

Harvey RP (1996). "NK-2 homeobox genes and heart development". Developmental Biology. 178 (2): 203–16.

Harvey RP. (2002). Patterning the vertebrate heart. Nat Rev Genet 3: 544–556.

Hashimoto H, Yuasa S, Tabata H, et al. (2014). Time-lapse imaging of cell cycle dynamics during development in living cardiomyocyte. J Mol Cell Cardiol. 72:241–249.

Hashimoto, H., Rebagliati, M., Ahmad, N., Muraoka, O., Kurokawa, T., Hibi, M., Suzuki, T. (2004). The Cerberus/Dan-family protein Charon is a negative regulator of Nodal signaling during left-right patterning in zebrafish. Development 131, 1741–1753.

Heikinheimo M, Scandrett JM, Wilson DB. (1994). Localization of transcription factor GATA-4 to regions of the mouse embryo involved in cardiac development. Dev Biol 164: 361–373

Hirokawa, N., Tanaka, Y., & Okada, Y. (2012). Cilia, KIF3 molecular motor and nodal flow. Current Opinion in Cell Biology, 24(1), 31–39.

Hirschy, A., Schatzmann, F., Ehler, E., Perriard, J., 2006. Establishment of cardiac cytoarchitecture in the developing mouse heart. Dev. Biol. 289, 430–441.

Hoffman JI (1995). Incidence of congenital heart disease. I: Postnatal incidence. Pediatr Cardiol 16: 103–113.

Hooghe B, Hulpiau P, Van Roy F and De Bleser PD (2008). ConTra: a promoter alignment analysis tool for identification of transcription factor binding sites across species. Nucleic Acids Res. 36:W128–W132.

Hutson MR, Kirby ML (2007). Model systems for the study of heart development and disease. Cardiac neural crest and conotruncal malformations. Semin Cell Dev Biol 18:101–110.

Ieda M, Tsuchihashi T, Ivey KN, Ross RS, Hong TT, Shaw RM, Srivastava D. (2009). Cardiac fibroblasts regulate myocardial proliferation through beta1 integrin signaling. Dev Cell. 16:233–244.

Ieda, M., Tsuchihashi, T., Ivey, K.N., Ross, R.S., Hong, T., Shaw, R.M., Srivastava, D. (2010). Cardiac Fibroblasts Regulate Myocardial Proliferation through β-1 Integrin Signaling. Dev. Cell 16, 233–244.

Inácio, J.M., Marques, S., Nakamura, T., Shinohara, K., Meno, C., Hamada, H., Belo, J.A. (2013). The dynamic right-to-left translocation of Cerl2 is involved in the regulation and termination of Nodal activity in the mouse node. PLoS One 8, e60406.

Johnson, M. H., & Ziomek, C. A. (1981). The foundation of two distinct cell lineages within the mouse morula. Cell, 24(1), 71–80.

Kaufman, MH.; Bard, JBL. The Anatomical Basis of the Mouse Development (1999). Academic Press; San Diego, CA.

Kawasumi, A., Nakamura, T., Iwai, N., Yashiro, K., Saijoh, Y., Belo, J.A., Shiratori, H., Hamada, H. (2011). Left-right asymmetry in the level of active Nodal protein produced in the node is translated into left-right asymmetry in the lateral plate of mouse embryos. Dev. Biol. 353, 321–330.

Kelley C, Blumberg H, Zon LI, Evans T. (1993). GATA-4 is a novel transcription factor expressed in endocardium of the developing heart. Development 118: 817–827.

Kelly RG. (2012). The second heart field. Curr Top Dev Biol 100: 33–65.

Kelly, R. G., Buckingham, M. E., & Moorman, A. F. (2014). Heart fields and cardiac morphogenesis. Cold Spring Harbor perspectives in medicine, 4(10), a015750.

Keyte A, Hutson MR. (2012). The neural crest in cardiac congenital anomalies. Differentiation 84: 25–40.

Kimelman D. Mesoderm induction: from caps to chips (2006). Nat. Rev. Genet. 7:360–372.

Kimura, C., Yoshinaga, K., Tian, E., Suzuki, M., Aizawa, S., and

Matsuo, I. (2000). Visceral endoderm mediates forebrain development by suppressing posteriorizing signals. Dev. Biol. 225, 304–321.

Kirby, M. L. (2007). Cardiac development. Oxford; New York: Oxford University Press.

Kitajima, K., Oki, S., Ohkawa, Y., Sumi, T., Meno, C. (2013). Wnt signaling regulates left –right axis formation in the node of mouse embryos. Dev. Biol. 380, 222–232.

Krupinski, P., Chickarmane, V., Peterson, C. (2011). Simulating the mammalian blastocyst-molecular and mechanical interactions pattern the embryo. PLoS Comput. Biol. 7,e1001128.

Kubalak SW, Miller-Hance WC, O'Brien TX, Dyson E, Chien KR. (1994). Chamber specification of atrial myosin light chain-2 expression precedes septation during murine cardiogenesis. J Biol Chem 269: 16961–16970.

Le, T., and Chong, J. (2017). Cardiac progenitor cells for heart repair. Cell Death Discov. 2, 1–4.

Li, F., Wang, X., Capasso, J.M., Gerdes, A.M., 1996. Rapid transition of cardiac myocytes from hyperplasia to hypertrophy during postnatal development. J. Mol. Cell. Cardiol. 28, 1737–1746.

Lints TJ, Parsons LM, Hartley L, Lyons I, Harvey RP. (1993). Nkx-2.5: A novel murine homeobox gene expressed in early heart progenitor cells and their myogenic descendants. Development 119: 969.

Liu Y, Semina EV (2012) pitx2 Deficiency Results in Abnormal Ocular and Craniofacial Development in Zebrafish. PLOS ONE 7(1): e30896.

Logan, M., Pagán-Westphal, S. M., Smith, D. M., Paganessi, L., & Tabin, C. J. (1998). The transcription factor pitx2 mediates situs-specific morphogenesis in response to left-right asymmetric signals. Cell, 94(3), 307–317.

Malumbres, M., Barbacid, M. Cell cycle, CDKs and cancer: a changing paradigm (2009). Nat Rev Cancer 9, 153–166.

Ma ZG, Yuan YP, Zhang X, Xu SC, Wang SS, Tang QZ (2017) Pip-erine Attenuates pathological cardiac fibrosis via PPAR-γ/AKT pathways. EBioMedicine18: 179–187.

Manner J, Perez-Pomares JM, Macias D, Munoz-Chapuli R. (2001). The origin, formation and developmental significance of the epicardium: A review. Cells Tissues Organs 169: 89–103.

Marikawa, Y., & Alarcon, V. B. (2012). Creation of trophectoderm, the first epithelium, in mouse preimplantation development. Results and problems in cell differentiation, 55, 165–184.

Marikawa, Y., Alarcón, V.B. (2010). Establishment of trophectoderm and inner cell mass lineages in the mouse embryo. Mol. Reprod. Dev. 76, 1019–1032.

Marques, S., Borges, A. C., Silva, A. C., Freitas, S., Cordenonsi, M., & Belo, J. A. (2004). The activity of the Nodal antagonist Cerl-2 in the mouse node is required for correct L/R body axis. Genes and Development, 18(19), 2342–2347.

Marvin MJ, Di Rocco G, Gardiner A, Bush SM, Lassar AB. (2001). Inhibition of Wnt activity induces heart formation from posterior mesoderm. Genes Dev 15: 316–327.

Mendis S, Puska P, Norrving B (2011). Global Atlas on Cardiovascular Disease Prevention and Control (PDF). World Health Organization in collaboration with the World Heart Federation and the World Stroke Organization. pp. 3–18. ISBN 978-92-4-156437-3. Archived (PDF) from the original on 2014-08-17.

Meno, C. et al. (1998). Lefty-1 is required for left–right determination as a regulator of lefty-2 and nodal. Cell 94, 287–297.

Meno, C. et al. (2001). Diffusion of nodal signaling activity in the absence of the feedback inhibitor Lefty2. Dev. Cell 1,127–138.

Meno, C., Ito, Y., Saijoh, Y., Matsuda, Y., Tashiro, K., Kuhara, S. and Hamada, H. (1997). Two closely related left-right asymmetrically expressed genes, lefty-1 and lefty-2: their distinct expression domains, chromosomal linkage and direct neuralizing activity in Xenopus embryos. Genes to Cells, 2: 513-524.

Meno, C., Takeuchi, J., Sakuma, R., Koshiba-Takeuchi, K., Ohishi, S., Saijoh, Y., Miyazaki, J., ten Dijke, P., Ogura, T., Hamada, H. (2001). Diffusion of nodal signaling activity in the absence of the feedback inhibitor Lefty2. Dev. Cell 1, 127–138.

Mikawa, T., Poh, A. M., Kelly, K. A., Ishii, Y. and Reese, D. E. (2004), Induction and patterning of the primitive streak, an organizing center of gastrulation in the amniote. Dev. Dyn., 229: 422-432.

Modlin IM, Moss SF, Chung DC, et al (2008). Priorities for improving the management of gastroenteropancreatic neuroendocrine tumors. J Natl Cancer Inst. 100:1282–1289.

Moran, A. E., Forouzanfar, M. H., Roth, G. A., Mensah, G. A., Ezzati, M., Flaxman, A., … Naghavi, M. (2014). The global burden of ischemic heart disease in 1990 and 2010: the Global Burden of Disease 2010 study. Circulation, 129(14), 1493–1501.

Nakamura, T., Hamada, H. (2012). Left-right patterning: conserved and divergent mechanisms. Development 139, 3257–3262.

Nakaya Y, Sheng G. (2008). Epithelial to mesenchymal transition during gastrulation: an embryological view. Dev. Growth Differ. 50:755–66

Nakaya Y, Sukowati EW, Wu Y, Sheng G. (2008). RhoA and microtubule dynamics control cell-basement membrane interaction in EMT during gastrulation. Nat. Cell Biol. 10:765–75

Naqvi, N., Li, M., Yahiro, E., Graham, R. M., & Husain, A. (2009). Insights into the characteristics of mammalian cardiomyocyte terminal differentiation shown through the study of mice with a dysfunctional c-kit. Pediatric cardiology, 30(5).

Nieto MA. (2011). The ins and outs of the epithelial to mesenchymal transition in health and disease. Annu. Rev. Cell Dev. Biol. 27:347–76

Noseda M, Peterkin T, Simoes FC, Patient R, Schneider MD (2011). Cardiopoietic factors: Extracellular signals for cardiac lineage commitment. Circ Res 108: 129–152.

P. Hydbring, M. Malumbres, P. Sicinski (2016). Non-canonical functions of cell cycle cyclins and cyclin-dependent kinases. Nat. Rev. Mol. Cell Biol., 17 (2016), pp. 280-292.

Pasumarthi, K.B.S., Field, L.J. (2002). Cardiomyocyte Cell Cycle Regulation. Circ. Res. 90, 1044–1054.

Pearce J.J., Penny, G., and Rossant, J. (1999). A mouse cerberus/Dan-related gene family. Dev Biol. 209: 98-110.

Pennisi, D.J., Ballard, V.L.T., Mikawa, T., 2003. Epicardium is required for the full rate of myocyte proliferation and levels of expression of myocyte mitogenic factors FGF2 and its receptor, FGFR-1, but not for transmural myocardial patterning in the embryonic chick heart. Dev. Dyn. 228, 161–172.

Perea-Gomez, A., Camus, A., Moreau, A., Grieve, K., Moneron, G., Dubois, A., Cibert, C., and Collignon, J. (2004). Initiation of gastrulation in the mouse embryo is preceded by an apparent shift in the orientation of the anterior-posterior axis. Curr. Biol. 14, 197–207.

Pérez-Pomares, J.M., González-Rosa, J.M., Muñoz-Chápuli, R., 2009. Building the vertebrate heart - an evolutionary approach to cardiac development. Int. J. Dev. Biol. 53, 1427–1443.

Place ES, Evans ND, Stevens MM. (2009). Complexity in biomaterials for tissue engineering. Nat Mater.8(6):457–70.

Quelle, D. E., Ashmun, R. A., Shurtleff, S. A., Kato, J. Y., Bar-Sagi, D., Roussel, M. F., & Sherr, C. J. (1993). Overexpression of mouse D-type cyclins accelerates G1 phase in rodent fibroblasts. Genes and Development, 7(8), 1559–1571.

Reese DE, Mikawa T, Bader DM. (2002). Development of the coronary vessel system. Circ Res 91: 761–768.

Reifers F, Walsh EC, Leger S, Stainier DY, Brand M. (2000). Induction and differentiation of the zebrafish heart requires fibroblast growth factor 8 (fgf8/acerebellar). Development 127: 225–235.

Ricard-Blum S (2001). The collagen family. Cold Spring Harb Perspect Biol. Jan 1; 3(1):a004978.

Rienks, M., Papageorgiou, A.-P., Frangogiannis, N. G., & Heymans, S. (2014). Myocardial Extracellular Matrix: An Ever-Changing and Diverse Entity. Circulation Research, 114(5), 872–888. doi:10.1161/circresaha.114.302533.

Risebro, C.A., Riley, P.R., 2006. Formation of the ventricles. Sci. World J. 6, 1862–1880.

Rodgers, L. S., Schnurr, D. C., Broka, D., & Camenisch, T. D. (2009). An improved protocol for the isolation and cultivation of embryonic mouse myocytes. Cytotechnology, 59(2), 93–102.

Rodriguez-Esteban, C., Tsukui, T., Yonei, S. et al. (1999) The T-box genes Tbx4 and Tbx5 regulate limb outgrowth and identity. Nature 398, 814–818.

Rumiantsev, P.P., Bruce, M.C. (1991). Growth and hyperplasia of cardiac muscle cells., in: London, U.K.: Harwood Academic Publishers.

Savolainen, S. M., Foley, J. F., & Elmore, S. A. (2009). Histology Atlas of the Developing Mouse Heart with Emphasis on E11.5 to E18.5. Toxicologic Pathology, 37(4), 395–414.

Schier, A.F. (2009). Nodal morphogens. Cold Spring Harb. Perspect. Biol. 1, a003459

Schneider VA, Mercola M. (2001). Wnt antagonism initiates cardiogenesis in Xenopus laevis. Genes Dev 15: 304–315.

Schultheiss TM, Burch JB, Lassar AB. (1997). A role for bone morphogenetic proteins in the induction of cardiac myogenesis. Genes Dev 11: 451–462.

Sedmera, D., Thompson, R.P. (2011). Myocyte proliferation in the developing heart. Dev. Dyn. 240, 1322–1334.

Shen, M.M. (2007). Nodal signaling; developmental roles and regulation. Development 134, 1023–1034.

Shiratori, H., & Hamada, H. (2014). TGF-β signaling in establishing left-right asymmetry. Seminars inCell and Developmental Biology, 32, 80–84.

Shiratori, H., Hamada, H. (2006). The left-right axis in the mouse): from origin to morphology. Development 133, 2095–2104.

Shiratori, H., Sakuma, R., Watanabe, M., Hashiguchi, H., Mochida, K., Sakai, Y., Nishino, J., Saijoh, Y., Whitman, M., Hamada, H. (2001). Two-step regulation of left-right asymmetric expression of Pitx2: initiation by nodal signaling and maintenance by Nkx2. Mol. Cell 7, 137–49.

Shirendeb U, Hishikawa Y, Moriyama S, et al (2009). Human papillomavirus infection and its possible correlation with p63 expression in cervical cancer in Japan, Mongolia, and Myanmar. Acta Histochem Cytochem. 42:181–190. 2009.

Soonpaa, M.H., Kim, K.K., Pajak, L., Franklin, M., Field, L.J. (1996). Cardiomyocyte DNA synthesis and binucleation during murine development. Am. Physiol. Soc. 271, H2183–H2189.

Sorimachi H, et al. (1997). Tissue-specific expression and α-actinin binding properties of the Z-disc titin: implications for the nature of vertebrate Z-discs1 Journal of Molecular Biology 270(5), 688-695.

Suckow, M., Danneman, P., & Brayton, C. (2001). The laboratory mouse. CRC Press LLC.

Takaoka, K., Hamada, H. (2012). Cell fate decisions and axis determination in the early mouse embryo. Development 139, 3–14

Takaoka, K., Yamamoto, M., Hamada, H. (2011). Origin and role of distal visceral endoderm, a group of cells that determines anterior-posterior polarity of the mouse embryo. Nat. Cell Biol. 13, 743–752.

Takeda K, Kishi H, Ma X, Yu ZX, Adelstein RS (2003). Ablation and mutation of nonmuscle myosin heavy chain II-B results in a defect in cardiac myocyte cytokinesis.Circ Res. 93:330–337.

Tam, P.P.L., Behringer, R.R. (1997). Mouse gastrulation: the formation of a mammalian body plan. Mech. Dev. 68, 3–25.

Ten Dijke, P., Hill, C.S. (2004). New insights into TGF-beta-Smad signalling. Trends Biochem. Sci. 29, 265–273.

Townsend, N., Wilson, L., Bhatnagar, P., Wickramasinghe, K., Rayner, M., & Nichols, M. (2016). Cardiovascular disease in Europe: epidemiological update 2016. European Heart Journal, 37(42), 3232-3245.

Toyoda M, Shirato H, Nakajima K, Kojima M, Takahashi M, Kubota M, Suzuki-Migishima R, Motegi Y, Yokoyama M, Takeuchi T. (2003). jumonji downregulates cardiac cell proliferation by repressing cyclin D1 expression. Dev Cell. 5:85–97.

Tzahor E, Lassar AB. (2001). Wnt signals from the neural tube block ectopic cardiogenesis. Genes Dev 15: 255–260.

Valenta, T.; Hausmann, G.; Basler, K. (2012). The many faces and functions of β-catenin. EMBO J. 31, 2714–2736.

van den Berg, G., Abu-Issa, R., de Boer, B.A., Hutson, M.R., de Boer, P.A., Soufan, A.T., Ruijter, J.M., Kirby, M.L., van den Hoff, M.J., Moorman, A.F. (2009). A caudal proliferating growth center contributes to both poles of the forming heart tube. Circ. Res. 104, 179–188.

Villarreal, F., Epperson, S. A., Ramirez-Sanchez, I., Yamazaki, K. G., & Brunton, L. L. (2009). Regulation of cardiac fibroblast collagen synthesis by adenosine: roles for Epac and PI3K. American journal of physiology. Cell physiology, 296(5), C1178–C1184. doi:10.1152/ajpcell.00291.2008.

Waldo KL, Hutson MR, Ward CC, Zdanowicz M, Stadt HA, Kumiski D, Abu-Issa R, Kirby ML. (2005). Secondary heart field contributes myocardium and smooth muscle to the arterial pole of the developing heart. Dev Biol 281: 78–90.

Walsh S, Ponten A, Fleischmann BK, Jovinge S (2010). Cardiomyocyte cell cycle control and growth estimation *in vivo*--an analysis based on cardiomyocyte nuclei. Cardiovas Res 86: 365–373. 10.1093/cvr/cvq005.

Watt AJ, Battle MA, Li J, Duncan SA. (2004). GATA4 is essential for formation of the proepicardium and regulates cardiogenesis. Proc. Nat. Acad. Sci. U.S.A. 101:12573–12578.

Wessels, A., Sedmera, D. (2003). Developmental anatomy of the heart: a tale of mice and man. Physiol. Genomics 15, 165–176.

Yamamoto, M., Saijoh, Y., Perea-Gomez, A. et al. (2004). Nodal antagonists regulate formation of the anteroposterior axis of the mouse embryo. Nature 428, 387–392.

Yoshioka, H., Meno, C., Koshiba, K., Sugihara, M., Itoh, H., Ishimaru, Y., … & Noji, S. (1998). Pitx2, a bicoid-type homeobox gene, is involved in a lefty-signaling pathway in determination of leftright asymmetry. Cell, 94(3), 299–305.

Zaffran S, Kelly RG, Meilhac SM, Buckingham ME, Brown NA. (2004). Right ventricular myocardium derives from the anterior heart field. Circ Res 95: 261–268.

Zaffran, S., Frasch, M., 2002. Early Signals in Cardiac Development. Circ. Res. 91, 457–469.

Zeisberg EM, Ma Q, Juraszek AL, Moses K, Schwartz RJ, Izumo S, Pu WT. (2005). Morphogenesis of the right ventricle requires myocardial expression of Gata4. J Clin Invest 115: 1522–1531.

Zhu, L., Marvin, M.J., Gardiner, A., Lassar, A.B., Mercola, M., Stern, C.D., Levin, M. (1999). Cerberus regulates left-right asymmetry of the embryonic head and heart. Curr. Biol. 9, 931–938.